How Did Early Earth Become Our Modern World?

Richard W. Carlson,[1] Edward Garnero,[2]
T. Mark Harrison,[3] Jie Li,[4] Michael Manga,[5]
William F. McDonough,[6] Sujoy Mukhopadhyay,[7]
Barbara Romanowicz,[5] David Rubie,[8]
Quentin Williams,[9] and Shijie Zhong[10]

[1]Department of Terrestrial Magnetism, Carnegie Institution of Washington, Washington, DC 20015; email: rcarlson@ciw.edu

[2]School of Earth and Space Exploration, Arizona State University, Tempe, Arizona 85287; email: garnero@asu.edu

[3]Department of Earth and Space Sciences, University of California, Los Angeles, California 90095; email: tmh@argon.ess.ucla.edu

[4]Department of Earth and Environmental Sciences, University of Michigan, Ann Arbor, Michigan 48109; email: jackieli@umich.edu

[5]Department of Earth and Planetary Science, University of California, Berkeley, California 94720; email: manga@seismo.berkeley.edu, barbara@seismo.berkeley.edu

[6]Department of Geology, University of Maryland, College Park, Maryland 20742; email: mcdonoug@umd.edu

[7]Department of Earth and Planetary Sciences, Harvard University, Cambridge, Massachusetts 02138; email: sujoy@eps.harvard.edu

[8]Bayerisches Geoinstitut, University of Bayreuth, 95440 Bayreuth, Germany; email: dave.rubie@uni-bayreuth.de

[9]Department of Earth Sciences, University of California, Santa Cruz, California 95064; email: qwilliams@pmc.ucsc.edu

[10]Department of Physics, University of Colorado, Boulder, Colorado 80309; email: shijie.zhong@colorado.edu

Abstract

Several features of Earth owe their origin to processes occurring during and shortly following Earth formation. Collisions with planetary embryos caused substantial melting of the growing Earth, leading to prolonged core formation, atmosphere outgassing, and deepening of the magma ocean as Earth grew. Mantle noble gas isotopic compositions and the mantle abundance of elements that partition into the core record this very early Earth differentiation. In contrast, the elements that are not involved in either core or atmosphere formation show surprisingly muted evidence of the fractionation expected during magma ocean crystallization, and even this minimal evidence for early intramantle differentiation appears to have been erased by mantle convection within ~1.5 billion years of Earth formation. By 4.36 Ga, Earth's surface and shallow interior had reached temperatures similar to those of the present Earth, and mantle melting, and perhaps plate subduction, was producing crustal rock types similar to those seen today. Remnants of early Earth differentiation may still exist in the deep mantle and continue to influence patterns of large-scale mantle convection, sequestration of some trace elements, geomagnetic reversals, vertical motions of continents, and hot-spot volcanism.

1. INTRODUCTION

This review examines the processes that assembled dispersed dust and gas in the solar nebula into a planet that could begin the type of geological processes and develop the structures that define Earth today. The data for this story of early Earth evolution derive from many sources: astronomical observations of other planetary systems; theoretical modeling of planet formation and differentiation; cosmochemical investigations of meteoritic materials presumed to be the building blocks of Earth; experimental studies of the properties of Earth materials at high pressures and temperatures; direct analysis of Earth rocks that retain a memory of events that occurred in the first 100 Ma of Earth history; and geophysical imaging of present-day structures inside the deep Earth coupled with geodynamic modeling that provides an interpretive framework for the origin, evolution, and potential role these structures play in influencing the geologic evolution of Earth's surface. In reviewing these constraints, we highlight the features of the modern Earth that clearly owe their origin to processes associated with Earth formation and discuss the evidence that more subtle features of Earth's composition and structure were either created or highly influenced by events occurring within the first 100–200 Ma of Solar System history.

2. INHERITED COMPOSITIONAL CHARACTERISTICS

A first-order feature of Earth is the one that distinguishes the terrestrial from the gas-giant planets: its deficiency in volatile elements, where, in this case, volatile means having a condensation temperature of <1,200 K from a gas of solar composition (e.g., Lodders 2003). The degree to which any given volatile element is depleted in Earth correlates with its condensation temperature from a
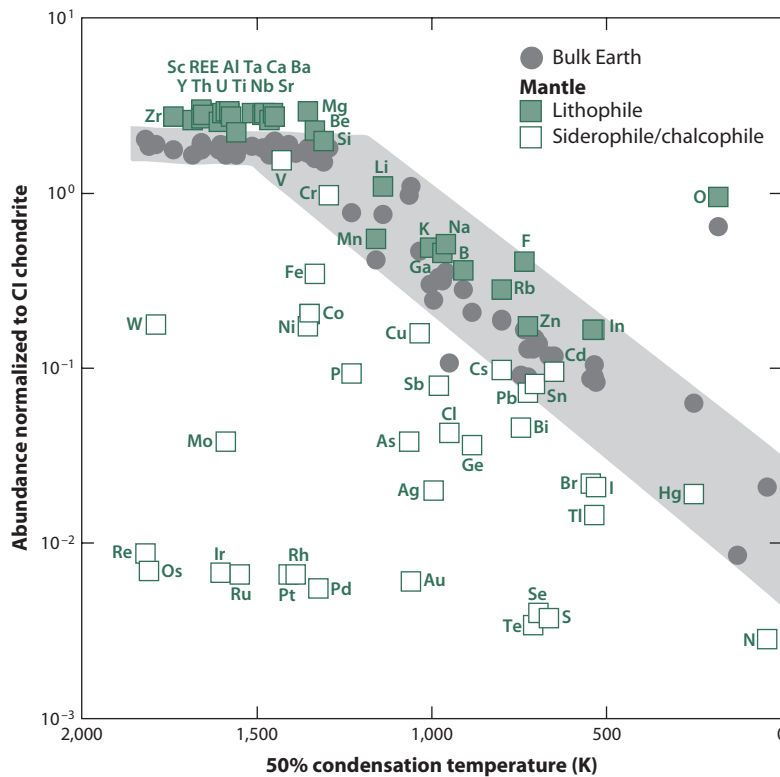
Figure 1

Element abundances in the bulk Earth (*gray circles*; McDonough 2003) and the mantle (Palme & O'Neill 2003) broken down into core-soluble (siderophile/chalcophile, *open green squares*) elements and core-insoluble (lithophile, *filled green squares*) elements, normalized by the average composition of the most volatile-rich type of primitive meteorite (CI chondrites) and Mg, against the temperature at which 50% of the element will be condensed from a gas of solar composition at 10 Pa or 10^{-4} atm. CI chondrite composition and condensation temperatures are from Lodders (2003). Abbreviation: REE, rare earth elements.

low-pressure gas of solar composition (**Figure 1**). The relative abundances in ancient Earth/Moon rocks of refractory ^{53}Cr (e.g., Lugmair & Shukolyukov 1998, Trinquier et al. 2008), derived in part from the 3.7 Ma half-life radioactive decay of moderately volatile ^{53}Mn, and refractory ^{87}Sr, derived from the 50 Ga half-life decay of volatile ^{87}Rb (Halliday & Kleine 2005), are lower than in most chondrites, which is indicative of the low Mn/Cr and Rb/Sr ratios of the volatile-depleted Earth. The deficiency in these isotopes dates Earth's volatile depletion to within 0 to 4 Ma of Solar System formation, implying that Earth grew from planetesimals that were already volatile depleted.

Fractionating volatile from refractory elements in the solar nebula is no surprise if most of Earth's mass derived from material condensed in the inner Solar System during a period when temperatures were high enough to limit the condensation of volatile elements to just their solubility in higher-temperature mineral phases. The presence of light noble gases of solar composition in Earth's interior (Harper & Jacobsen 1996, Pepin & Porcelli 2002, Yokochi & Marty 2004, Mukhopadhyay 2012) indicates that Earth did incorporate at least some, albeit likely a minor, component of even highly volatile elements collected from the solar nebula.

More contentious are the questions of whether other compositional gradients may have existed in the solar nebula and whether these could be preserved through the planetary accumulation
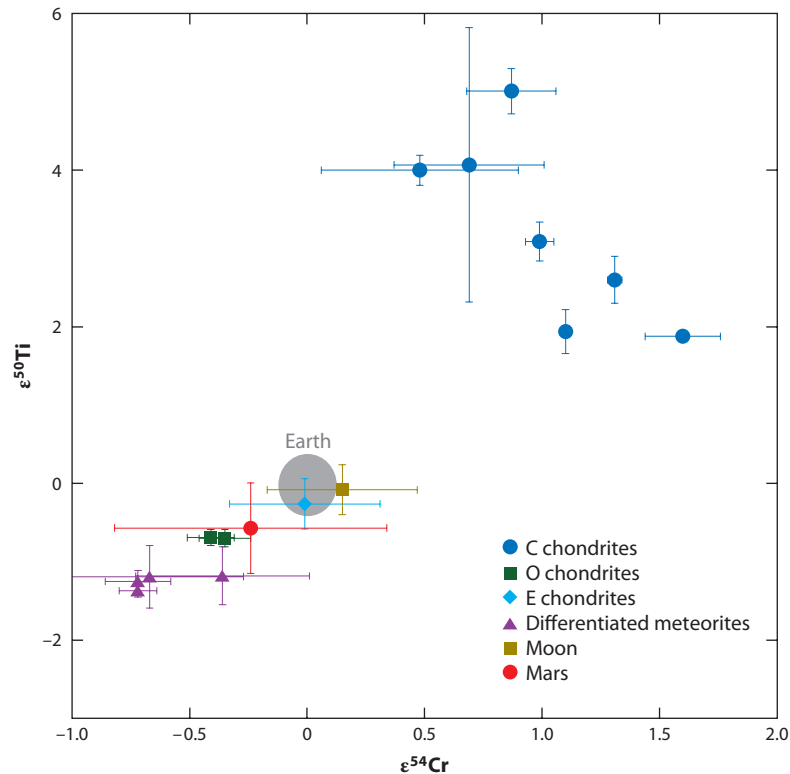
Figure 2

Nucleosynthetic variability in $^{50}Ti/^{47}Ti$ (Trinquier et al. 2009) and $^{54}Cr/^{52}Cr$ (Trinquier et al. 2007, Qin et al. 2010). $\varepsilon^{50}Ti = [(^{50}Ti/^{47}Ti)_{Sample}/(^{50}Ti/^{47}Ti)_{Standard} - 1] \times 10,000$, and $\varepsilon^{54}Cr = [(^{54}Cr/^{52}Cr)_{Sample}/(^{54}Cr/^{52}Cr)_{Standard} - 1] \times 10,000$, where the standards are terrestrial Ti and Cr. Similar isotopic distinctions between different meteorite groups and Earth are seen in Ni (Regelous et al. 2008), Mo (Dauphas et al. 2002, Burkhardt et al. 2011), Ru (Fischer-Godde et al. 2013), Ba, and Nd (Andreasen & Sharma 2007, Carlson et al. 2007). These isotopic differences between the meteorite parent bodies and Earth reflect different mixtures of the various nucleosynthetic components present in the solar nebula at the time of planet formation.

process. The most obvious evidence for the presence of an imperfectly mixed inner nebula is the observed isotopic variability in an increasing number of elements between the Earth/Moon system and other planetary objects including meteorites and Mars (Clayton et al. 1973, Dauphas et al. 2002, Carlson et al. 2007, Trinquier et al. 2007, Burkhardt et al. 2011, Warren 2011). The oxygen isotope composition of the Sun, as recently measured from implanted solar wind in the Genesis spacecraft (McKeegan et al. 2011), is extremely enriched in ^{16}O compared to that of Earth. This difference in the isotopic composition of Earth's second most abundant element reinforces the increasing evidence that Earth did not form from a mixture of nebular components equal to the average composition of the Solar System.

The observed stable isotope differences between most meteorite groups and Earth rule out carbonaceous chondrites as the primary building blocks of Earth (**Figure 2**). Most other meteorite groups also show isotopic distinctions from Earth, with one exception: the enstatite chondrites. Although they overlap Earth in the stable isotopic composition of many elements, enstatite chondrites are compositionally very different from upper mantle rocks, particularly in their very low

Table 1   Estimates of bulk silicate Earth (BSE) composition

	BSE (McDonough & Sun 1995)	BSE (Palme & O'Neill 2003)	BSE (Lyubetskaya & Korenaga 2007)	BSE[a] (Javoy et al. 2010)	Upper mantle[b] (Javoy et al. 2010)	Lower mantle[b] (Javoy et al. 2010)
SiO_2	45.0	45.4	45.0	49.8	45.8	51.8
MgO	37.8	36.8	39.5	36.5	39.0	35.3
FeO	8.04	8.10	7.97	8.84	7.94	9.28
Al_2O_3	4.43	4.49	3.52	2.42	3.59	1.85
CaO	3.53	3.65	2.79	1.87	2.73	1.46
Al/Si	0.11	0.11	0.089	0.053	0.089	0.040
Mg/Si	1.04	1.08	1.13	0.79	1.10	0.88
K (μg/g)	240	260	190	120	180	90
Th (ng/g)	80	83	63	44	67	33
U (ng/g)	20	22	17	12	18	9

[a]BSE based on an enrichment factor of 1.5 relative to CI and $K/U = 10^4$.

[b]Upper and lower mantle trace element compositions calculated assuming U (ng/g) / Al_2O_3 (wt%) = 4.95, Th/U = 3.7, and $K/U = 10^4$.

Mg/Si ratio, depletion in refractory elements relative to Mg, and high concentrations of some moderately volatile elements such as Na and S compared with other meteorite groups and Earth (Palme & O'Neill 2003). The isotopic results have reopened a long-running debate (Herndon 1979, Javoy 1995) about whether carbonaceous or enstatite chondrites serve as better reference points to model the bulk composition of Earth. If the bulk Earth indeed is similar in composition to enstatite chondrites, given that the composition of the upper mantle is relatively well known (McDonough & Sun 1995), the lower mantle must have a dramatically different major element composition (**Table 1**) with substantially higher SiO_2 and less than half the Al_2O_3 and CaO contents of the upper mantle (Javoy et al. 2010). The resolution of this issue is critical both for our understanding of bulk Earth composition and for solid Earth dynamics and thermal evolution because bulk Earth composition estimates that derive from carbonaceous chondrite models predict 60–80% higher abundances of the radioactive heat-producing elements U and Th compared with those predicted by models based on enstatite chondrites, and up to a factor of 2.4 difference in the U concentration in the lower mantle (**Table 1**) (Sramek et al. 2013).

In the end, however, using any single meteorite type to model bulk Earth composition ignores the fact that most planetary accumulation models predict that the materials that accrete into a planet derive from a wide variety of heliocentric distances and hence may include materials that span, or exceed, the compositional range seen in the available meteorite collection. Theoretical studies of planetesimal accumulation show that at least a fraction of whatever compositional heterogeneity was present initially in the solar nebula likely will be preserved through the accretion process (Chambers 2004). Several planetary accumulation models predict that the amount of volatile-rich, oxidized, outer Solar System material brought into the terrestrial planet–forming region increased in the latter stages of planet formation (O'Brien et al. 2006, Walsh et al. 2011). This provides support for heterogeneous Earth accretion models proposed on the basis of bulk Earth chemistry (Wanke et al. 1984), core-mantle element partitioning (Rubie et al. 2011), and short-lived isotope systematics sensitive to core formation and volatile addition (Schonbachler et al. 2010, Mukhopadhyay 2012, Peto et al. 2013).

2.1. Growing Earth from Already Differentiated Planetesimals

Modern planetary accumulation models (Thommes et al. 2003, Chambers 2004) predict that Earth likely formed from the accumulation of a mixture of a large number of small (tens to hundreds of kilometers in diameter) planetesimals and a smaller number, but possibly a larger mass proportion, of Moon- to Mars-sized planetary embryos. The record preserved in meteorites shows clearly that planetesimal-scale melting, likely driven by the heat released by the 730,000 year half-life radioactive decay of ^{26}Al, caused segregation of metallic cores and silicate mantles/crusts on these bodies within 1 to 3 Ma of Solar System formation (Lugmair & Shukolyukov 1998, Amelin 2008, Trinquier et al. 2008, Kleine et al. 2009). The maximum size for such quickly formed planetesimals might be inferred from Mars, where Hf-W isotope data imply that Mars reached approximately half of its current mass within 1.8 ± 1 Ma of Solar System formation (Dauphas & Pourmand 2011).

   Why does this matter for Earth? First, "global" melting on small planetesimals would have transferred volatile elements through volcanism from the planetesimal interior to the surface, where the more volatile elements would have been lost by gravitational escape. Accumulation of these volatile-depleted planetesimals into a growing Earth could then explain the evidence discussed above that Earth's deficiency in volatile elements was a characteristic of the planet essentially from the time of its formation. Second, during this early phase of planetary accumulation, energetic impacts between planetesimals likely were common. Impacts between differentiated planetesimals can produce fragments enriched in crust, mantle, or iron cores (Asphaug et al. 2005). If not all fragments recombine following collisions, then the accumulating material may well not reflect the average composition of the planetesimals. This type of collisional erosion might explain the unusually high iron metal–to–silicate ratio for Mercury (Benz et al. 1988). A more subtle expression may be a slight deficiency in Earth's accessible mantle of the elements that partition into melts during partial melting as a result of the preferential collisional erosion of the crusts of the differentiated planetesimals that accumulated to form Earth (Boyet & Carlson 2005, O'Neill & Palme 2008, Jackson et al. 2010).

2.2. Giant Impacts

One example of collisional erosion is Earth's Moon; most formation models now suggest that the Moon is made up of materials ejected from the proto-Earth's mantle during an impact with a large planetary embryo (Stevenson 1987). The giant-impact model for lunar origin is driven in part by compositional similarities between Earth and the Moon, for example in oxygen and titanium isotopic composition (Wiechert et al. 2001, Zhang et al. 2012), and by the fact that the bulk Moon has a low iron concentration (e.g., Wanke et al. 1973), which suggests that it formed from a planet/planetesimal that had already separated a core. An important constraint on models for the impact origin of the Moon is the need to explain the current angular momentum of the Earth-Moon system. This constraint caused early attempts to model Moon formation through a giant impact to focus on glancing blows by the impactor. In these models, the resulting Moon is composed primarily of material deriving from the impactor, not the proto-Earth (Canup 2004). Unless the impactor and proto-Earth had very similar compositions, these models do not satisfy the observed compositional similarity of Earth and the Moon unless some mechanism of postimpact equilibration is assumed (Pahlevan & Stevenson 2007). Two recent giant-impact models explore the possibility that angular momentum in the Earth-Moon system can be lost through an orbital resonance between the Sun, Earth, and Moon. Relaxing the constraint imposed by the Earth-Moon angular momentum allows other impact scenarios, for example between a Moon-sized impactor and a fast-spinning Earth (**Figure 3**) (Cuk & Stewart 2012) or between two half–Earth mass

embryos (Canup 2012), to produce a debris disk composed either mostly of the proto-Earth or of such an intimate mixture of Earth and impactor that the resulting Moon would be compositionally similar to Earth.

Although giant impacts are expected phenomena during planetary accumulation, and may be repeated several times during the early history of a planet, the Moon-forming impact may represent the last giant impact in Earth history. Dating the time of this impact has not proven easy. Ages of the oldest lunar crustal rocks (Nemchin et al. 2008, Taylor et al. 2009, Borg et al. 2011) and model ages for the chemical differentiation of the lunar interior (e.g., Tera & Wasserburg 1974, Carlson & Lugmair 1979, Nyquist & Shih 1992, Touboul et al. 2007, Taylor et al. 2009) suggest Moon formation ages of 4.4 to 4.45 Ga that are surprisingly late compared with the expectation from most accretion models. Perhaps reflecting the consequences of this giant impact on Earth evolution, broadly similar ages are obtained from U-Pb and I-Xe model ages for Earth's mantle (Allegre et al. 2008, Mukhopadhyay 2012), ^{146}Sm-^{142}Nd model ages for the mantle sources of some ancient terrestrial crustal rocks (Boyet et al. 2003, Caro et al. 2006, Rizo et al. 2011), and the ages of the oldest crustal materials on Earth (Wilde et al. 2001, O'Neil et al. 2012).

3. DIFFERENTIATION OF THE EARLY EARTH

3.1. Magma Oceanography

The energy of a Moon-forming impact is sufficient to cause large degrees of melting of the solid Earth (Tonks & Melosh 1993). Because impacts of this size are common during planetary accretion, there is a reasonable expectation that planet growth may include several magma ocean episodes. Almost immediately after the return of the first Apollo samples from the Moon, a lunar magma ocean was invoked to explain the presence of a global, nearly monomineralic, anorthositic crust (e.g., Wood et al. 1970) and the complementary depletion of the mantle source of some mare basalts in Eu, the only rare earth element that is strongly enriched in the anorthite feldspar of the lunar crust (e.g., Taylor & Jakes 1974). Isotopic data confirm that these compositional characteristics were established shortly after Moon formation (Carlson & Lugmair 1979, Nyquist et al. 1995, Boyet & Carlson 2007, Brandon et al. 2009). Similarly, extreme isotopic variation in young basalts from Mars shows that global differentiation of the interior of Mars occurred within tens of millions of years of its formation (e.g., Borg & Draper 2003, Dauphas & Pourmand 2011). As is discussed in detail in this section, there is clear evidence on Earth for rapid core formation (Kleine et al. 2009), for the removal of core-soluble elements from the mantle, and for outgassing of noble gases from the mantle (e.g., Pepin 1991, Peto et al. 2013). Evidence of the type of extreme differentiation of the silicate portion of Earth similar to that observed on the Moon and Mars is surprisingly muted. Why might this be?

A terrestrial magma ocean may solidify in a rather different manner from those on smaller planetary bodies such as Mars and the Moon, where the pressure range is many times smaller. A magma ocean begins to crystallize at the depth where its liquidus intersects the adiabat, assuming the melt is vigorously convecting and hence well mixed. As illustrated in **Figure 4**, in a shallow magma ocean, or on a small planet(esimal), where the basal pressure stays below ~30 GPa, the magma ocean solidifies from the bottom upward. Within this pressure range, the adiabatic temperature gradient is smaller than that of the liquidus, and therefore the two curves intersect at the high-pressure end. For a magma ocean that extends to more than ~70 GPa, solidification may initiate in the middle where the adiabat just touches the liquidus at an intermediate depth, with crystallization proceeding to both greater and lesser depth as cooling continues. For their chondritic composition, however, Andrault et al. (2011) found that the liquidus increased nearly
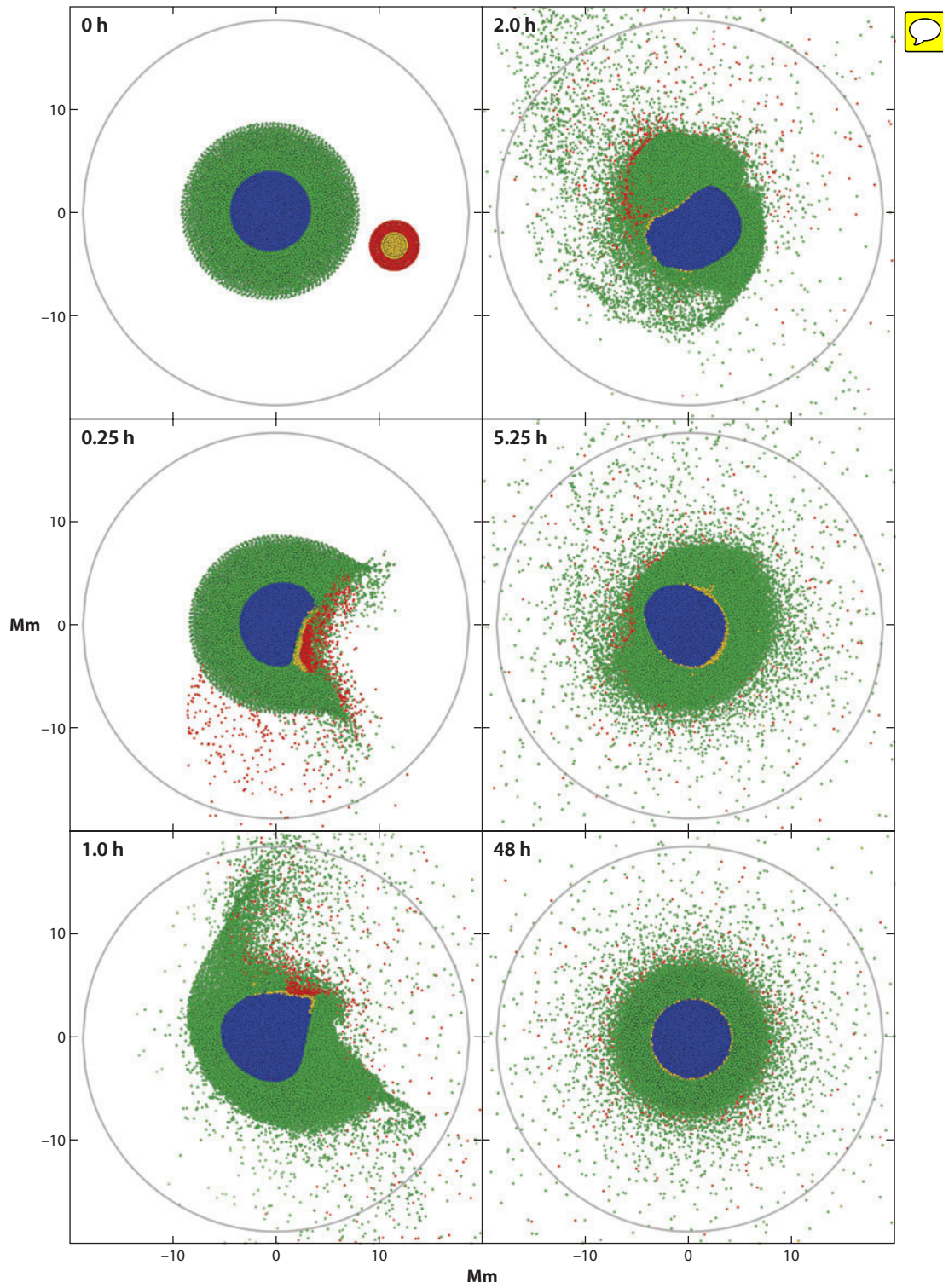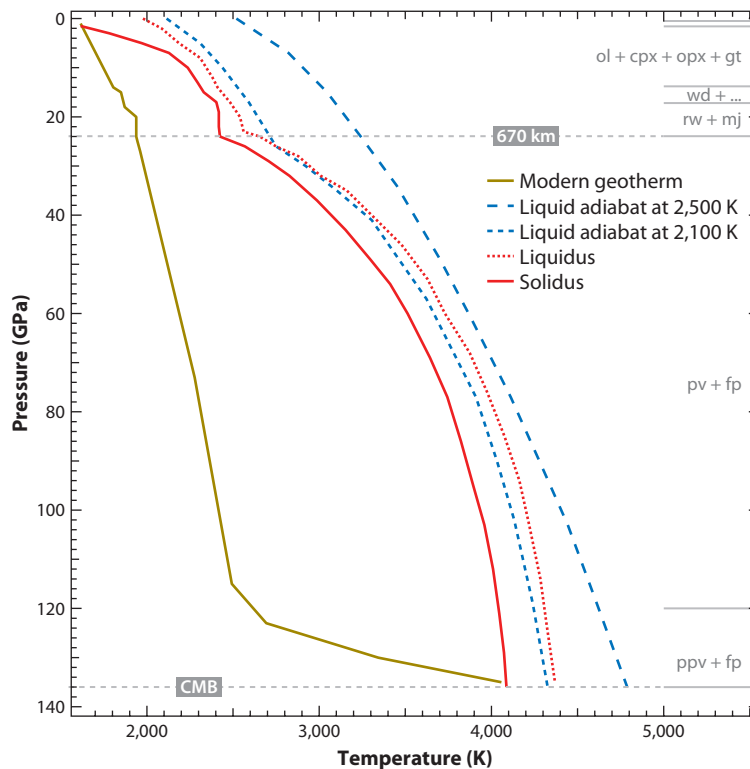
Figure 4

Temperature profiles that determine the crystallization conditions of a Hadean magma ocean, after Stixrude et al. (2009). The dark yellow solid curve is the modern mantle geotherm; the red dotted and solid curves are the mantle liquidus and solidus temperature profiles, respectively; the blue dashed lines are the mantle adiabatic temperature profiles at 2,500 and 2,100 K. Marked along the vertical axis are liquidus phases of bulk silicate Earth within different pressure ranges, after Elkins-Tanton (2012): cpx, clinopyroxene $Ca(Mg,Fe)Si_2O_6$; fp, ferropericlase $(Mg,Fe)O$; gt/mj, garnet/majorite $Mg_3Al_2Si_3O_{12}$; ol/rw/wd, olivine/ringwoodite/wadsleyite $(Mg,Fe)_2SiO_4$; opx, orthopyroxene $(Mg,Fe)SiO_3$; ppv/pv, postperovskite/perovskite $(Mg,Fe)(Si,Al)O_3$. Garnet is replaced by spinel $MgAl_2O_4$ between 0.5 and 1.6 GPa, and by plagioclase $Ca(Al)Si_2O_8$ between the surface and 0.5 GPa. Abbreviation: CMB, core-mantle boundary.

linearly with pressure throughout the depth range of the mantle. In this case, the magma ocean adiabat intersects the liquidus curve at the base of the mantle.

The manner in which a magma ocean crystallizes will have dramatic consequences for the time required for its solidification. In the case of bottom-up crystallization, and without either an insulating crust or thick atmosphere, a deep terrestrial magma ocean could solidify quickly, in less than

Figure 3

Example of an impact into a rapidly spinning Earth that causes ejection of enough terrestrial material to form the Moon. Shown is a view of the lower hemisphere of the impact event, where the colors denote materials. The mantle and core of the proto-Earth (*green* and *blue*, respectively) and of the impactor (*red* and *yellow*, respectively) are tracked through the simulation. In this hydrocode calculation (Cuk & Stewart 2012), the impactor is 0.05 times the mass of Earth and impacts at 20 km/s onto a proto-Earth spinning with a 2.3-h period. The Moon accretes from the circumterrestrial disk just beyond the Roche radius (*gray circles*).
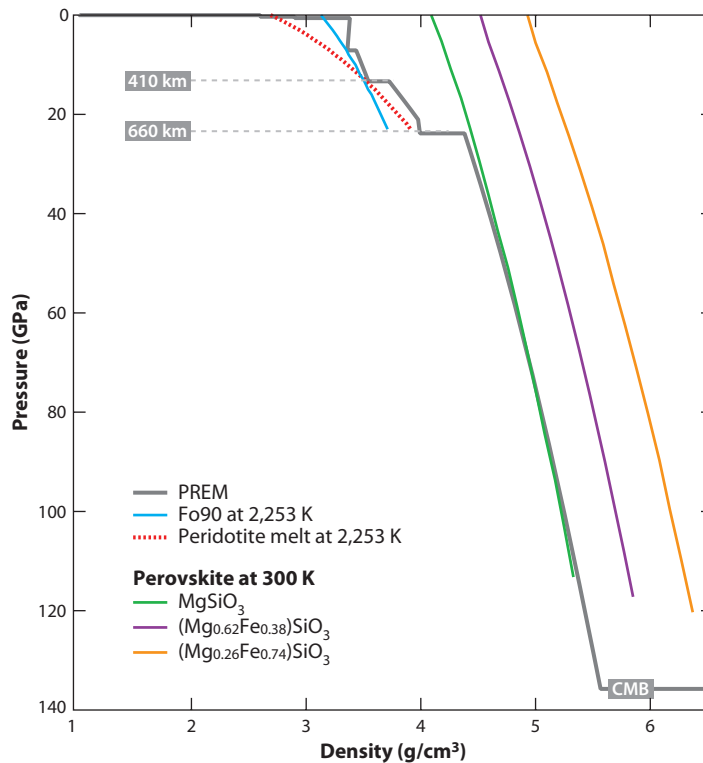
Figure 5

Density profiles of solid and liquid phases in the mantle in comparison with the Preliminary Reference Earth Model (PREM; Dziewonski & Anderson 1981). Those of olivine with an Mg# of 90 (Fo90) and of peridotite melt are from Lee et al. (2010), and they show a crossover in density between solid and melt under elevated pressure. Densities of perovskites with variable amounts of Fe end-member (0%, 38%, and 74% in mole fraction) at 300 K are according to Dorfman et al. (2013), to show the effect of iron content on the density. Abbreviation: CMB, core-mantle boundary.

a thousand (Solomatov 2000) to a million (Elkins-Tanton 2008) years. In contrast, a basal magma ocean separated from the surface could survive for most of Earth history (Labrosse et al. 2007).

One of the key uncertainties in understanding the consequences of a magma ocean for mantle composition and thermal evolution is thus its depth. Several lines of evidence have been invoked to add constraints on this parameter. One involves the pressures and temperatures needed to explain the magnitude of depletion of the elements that preferentially partition into iron metal during core formation, as discussed in Section 3.2. This path implies magma ocean pressures of order 40–60 GPa, or depths of ∼1,000–1,500 km (Bouhifd & Jephcoat 2011, Burkemper et al. 2012, Seibert et al. 2013). This approach may determine a shallower limit on the depth extent of an early magma ocean, and clearly indicates that lower mantle mineral assemblages (**Figure 5**) are critical in the phase equilibria of a deep magma ocean.

An observational rationale for invoking a much deeper early magma ocean, extending to the base of the mantle, is the presence of ultralow-velocity zones (ULVZ) at the base of Earth's mantle: thin (∼5–40 km thick) regions that have been associated with partial melting of silicates directly above the core (Williams & Garnero 1996, Lay et al. 2004, Rost et al. 2005, McNamara et al. 2010). Thermal and geochemical arguments associate these regions with the last residue of

a fractionally crystallizing deep magma ocean (Labrosse et al. 2007, Coltice et al. 2011). Unless the mantle solidus is markedly lowered by volatiles and/or core contamination, the temperature needed to melt to the base of the mantle may be in excess of 4,000 K (Fiquet et al. 2010, Andrault et al. 2012, Liebske & Frost 2012). This may have important consequences for the suggested presence in the lowermost mantle of the newly discovered postperovskite phase, as its stability field would lie at higher pressures than those at the base of the mantle (Catalli et al. 2009), in which case it may play little or no role in the geochemical evolution of a terrestrial magma ocean.

The uncertainties involved in the crystallization of a deep early magma ocean are profound and include (*a*) the depth extent of the magma ocean, (*b*) the loci of first crystallization, and (*c*) the style of crystallization (whether through fractional or equilibrium crystallization). The liquidus phase throughout the bulk of the lower mantle is magnesian perovskite for both peridotitic and chondritic compositions (Fiquet et al. 2010, Andrault et al. 2011). (Mg,Fe)O appears to be the solidus phase within peridotite at mid- to deep lower mantle conditions, whereas measurements are ambiguous as to whether $CaSiO_3$ or (Mg,Fe)O is the solidus phase within chondritic material (Fiquet et al. 2010, Andrault et al. 2011). Hence, if melting extended into the mid- to deep lower mantle, the initial crystallizing phase would be perovskite. Both Ca- and Mg-perovskite strongly fractionate rare earth elements from high-field-strength elements such as Nb and Hf (Corgne et al. 2005). Consequently, perovskite fractionation would rapidly change such ratios as Sm/Hf, yet the Sm/Hf ratio is relatively invariant in modern mid-ocean ridge basalts (MORBs) at 1.33 (Salters & Stracke 2004), only slightly lower than the chondritic ratio of 1.43, which limits the amount of perovskite fractionation to less than 10–15% (Corgne et al. 2005, Liebske et al. 2005). Perovskite also would fractionate Sm/Nd and Lu/Hf ratios in opposite directions, yet for most of Earth history, Nd and Hf isotope evolution are strongly correlated (Vervoort & Blichert-Toft 1999). Only in the most ancient crustal rocks do Hf diverge from Nd isotope compositions, perhaps reflecting a memory of the early phase of mantle differentiation when minor perovskite fractionation indeed may have occurred (Caro et al. 2005, Rizo et al. 2011).

Regardless of where initial crystallization of a magma ocean commences, the initially crystallizing perovskite is likely to be negatively buoyant (Funamori & Sato 2010, Thomas et al. 2012, de Koker et al. 2013). Whether or not this initially crystallizing perovskite would sink (if crystallizing in the mid-lower mantle) and hence fractionate from the residual magma is less clear. Within a vigorously convecting magma ocean, long-term convective entrainment of particles is likely. Solomatov (2007) calculated a critical crystal size within a magma ocean to be near 1 mm in order for crystal-liquid separation to occur. As this size is large, but not unreasonable, for mantle minerals, whether crystals separated from residual liquids during magma ocean crystallization is not clear. If the crystals did not separate from the remaining liquid, then the solidified mantle would have the same composition as the starting magma ocean.

Although there is agreement that initially crystallizing perovskite is negatively buoyant with respect to the melt, if the perovskite is removed, the remaining liquid will evolve to a composition that has a substantially higher density. Two parameters are of primary importance in determining the buoyancy of melts relative to the prevalent lower mantle phases, and particularly the most plausible liquidus phase, magnesian perovskite: (*a*) the intrinsic density change on fusion and (*b*) the iron partitioning between liquid and solid. Subsidiary chemical effects, such as the silica, Ca, Al, alkali, and volatile contents of the liquid, doubtless play a role in buoyancy as well, but these effects are ill constrained at this juncture. With respect to the intrinsic density change on fusion, the limited data for relevant end-member oxides at deep mantle pressures (MgO, $MgSiO_3$, and SiO_2; e.g., Funamori & Sato 2010) do not provide compelling evidence that volume increases on fusion. Density changes for fusion under deep mantle conditions are uncertain, but are typically of

order 5% or less and notably decrease at pressures approaching those at the core-mantle boundary (e.g., Mosenfelder et al. 2009, Stixrude et al. 2009).

Iron partitioning matters because the abundance of iron strongly influences the density of the melt. The partitioning of iron between silicate perovskite and coexisting melt is controversial, with results on olivine compositions yielding a marked shift in the partition coefficient (D = concentration of Fe in solid/concentration of Fe in liquid) of iron near 76 GPa, from values of $\sim$0.2 to 0.04—an amount sufficient to produce markedly iron-enriched melts above this pressure (Nomura et al. 2011). Such iron-rich melts would be negatively buoyant and hence could provide a possible explanation for the ULVZs at the base of the mantle. In contrast, Andrault et al. (2012) found D values of 0.6 to 0.47 over a similar pressure range in a chondritic mantle composition and attributed the large difference between their results and those of Nomura et al. (2011) to the presence of aluminum within their more compositionally complex experimental charges. The net result of such higher iron partition coefficients is that negatively buoyant melts would be difficult to generate via fractional crystallization processes, which would serve to make crystal-liquid separation inefficient and hence minimize chemical fractionation during magma ocean crystallization.

3.2. Core Formation Throughout Accretion of Earth

The most convincing evidence for a terrestrial magma ocean comes from the elements that are more soluble in iron metal than in silicate, the so-called siderophile elements. As shown in **Figure 1**, many siderophile elements are strongly depleted in the mantle. If this depletion reflects extraction of these elements into the core, the degree of depletion of an individual element M depends on its metal-silicate partition coefficient $D^{m-s}(M)$, which depends in turn on pressure, temperature, oxygen fugacity (fO$_2$), and for some elements the compositions of the metal and silicate phases. Partition coefficients, determined experimentally, can thus be used to constrain the pressure-temperature-fO$_2$ conditions under which metal and silicate equilibrated during core formation. The consensus at the present time is that metal-silicate equilibration at high pressures (e.g., 40–60 GPa) was required to produce the observed siderophile element depletions.

Formation of Earth's core required Fe-rich metal to separate efficiently from the silicate mantle over a length scale $>10^3$ km. For this to occur, at least the metal must be molten (Stevenson 1990). There are three possible segregation mechanisms: (*a*) the percolation of liquid Fe through a solid crystalline silicate aggregate, (*b*) sinking of large (kilometer-sized) liquid metal diapirs though crystalline silicate mantle, and (*c*) sinking and segregation of dispersed liquid iron droplets in a deep magma ocean. According to numerous experimental studies performed up to 25 GPa, mechanism *a* would result in significant amounts of metal being stranded in the silicate mantle and is therefore extremely inefficient. Mechanism *b* may well have operated but would not have resulted in significant chemical equilibration between metal and silicate because diffusion distances would be too short in comparison with the size of the sinking metal diapir. Mechanism *c* requires large-scale melting (i.e., deep magma ocean formation). Large-scale melting of metal and silicate allows fast and efficient segregation of these phases to form the core and mantle. Provided the metal is present as dispersed centimeter-sized droplets, chemical equilibration at high pressures and temperatures is readily achieved (Rubie et al. 2003).

Interpretations of experimental studies of the partitioning of siderophile elements between liquid iron and silicate often assume that core formation occurred at a specific temperature, pressure, and oxygen fugacity. In some cases, authors have argued that core formation was a single event with core and mantle equilibrating at one specific pressure, temperature, and oxygen fugacity

(Righter 2011). As determined equilibration pressures are typically within the range 40–60 GPa, the core and mantle would have had to equilibrate at a depth of ∼1,200 km when Earth was almost fully accreted; physically and chemically, this is extremely unlikely, if not impossible. An alternative and more realistic interpretation is that the determined set of conditions for core-mantle equilibration represents an average of a broad range of pressures and temperatures. Thus, Wade & Wood (2005) proposed a model of continuous core formation wherein each incoming planetesimal added to Earth throughout accretion segregated small amounts of core-forming metal to gradually grow the core. As Earth accreted and increased in size, a global magma ocean deepened, and pressures and temperatures of metal-silicate equilibration increased. This model gives results for a significant number of siderophile elements that are consistent with observed mantle concentrations provided the oxygen fugacity increases by ∼3 log units during accretion and core separation.

A recent model of multistage core formation in Earth is based on an idealized accretion scenario in which impactors progressively grow in size and have a mass of approximately 10% of Earth's mass at the time of each impact (Rubie et al. 2011). Thus, magma oceans become deeper and metal-silicate equilibration pressures become higher with time, as in Wade & Wood (2005). A unique feature of this model is that the bulk composition of the accreting material is defined, including its oxygen content. Results of this model suggest that accretion of Earth was heterogeneous, with the initial 60–70% of Earth's mass forming from highly reduced material and the final 30–40% from relatively oxidized material. The reduced material is assumed to have been depleted in volatile elements, whereas the more oxidized material was rich in ices, and hence volatile elements, and originated relatively far from the Sun, where temperatures were lower.

3.3. Late Additions and the End of Core-Mantle Exchange

A key observation that drove much of the effort described in the above section involves the group of elements known as the highly siderophile elements (HSEs: Pt, Pd, Ru, Rh, Ir, Os, Au, and Re). These elements have low-pressure metal-silicate distribution coefficients of 10^5 or higher, yet they are present in Earth's mantle at concentrations of only a bit less than 1% of those of chondritic meteorites (**Figure 1**). Furthermore, their abundances relative to one another in the mantle are similar to their relative abundances in chondrites, although in detail there are small differences (Walker 2009). Measurements at higher pressures and temperatures have not yet produced metal-silicate partition coefficients for these elements that would allow their mantle abundances to be reconciled with core-mantle equilibrium (Brenan & McDonough 2009, Mann et al. 2012).

Mantle HSE abundances have long been used to suggest that a small amount of chondritic material, the so-called late veneer, was added to Earth's mantle after core formation was complete (Chou et al. 1983). Evidence from invariant ratios of siderophile to lithophile elements in the mantle over at least the last 3 Ga of Earth history (**Figure 6**) limits the amount of core-mantle exchange to at most a few percent, and more likely less than a few tenths of a percent (Jochum et al. 1993, McDonough & Sun 1995, Brandon & Walker 2005). If the mantle was completely stripped of Ir by core formation, 2.6×10^{25} g of chondrite (0.4% of the mass of Earth) added to the mantle can produce the Ir concentrations observed in the mantle (3.2 ppb; Morgan et al. 2001).

For most other elements, such small amounts of late-accreting material would have little effect on bulk Earth composition, the exception being volatile elements, including water and sulfur. If the late veneer were compositionally like volatile-rich CI chondrites that contain 2 wt% hydrogen (Wasson & Kallemeyn 1988), 0.5% of an Earth's mass of CI chondrite could have supplied not only the HSE abundances of the mantle but also all the water present in the modern oceans (Wanke
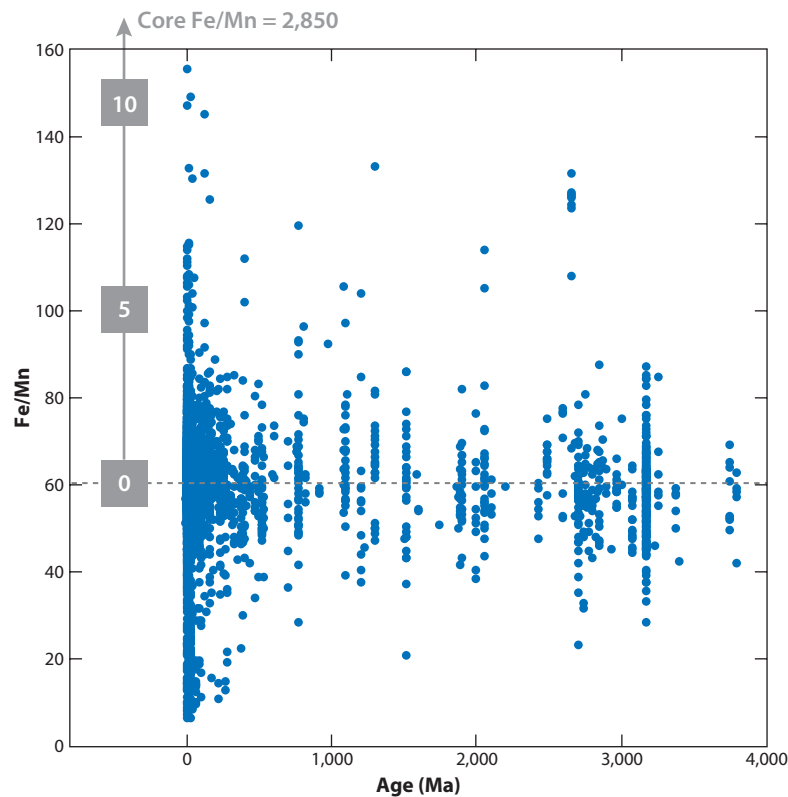
Figure 6

Ratio of Fe to Mn concentration in mafic volcanic rocks (8% < MgO <20%) throughout Earth history. Fractionation of the melts causes the range in Fe/Mn ratio seen at any one time, but the figure shows no obvious secular trend in Fe/Mn ratio that would suggest the addition or subtraction of high-Fe/Mn-ratio (2,850; McDonough 2003) core material to/from the mantle. The vertical bar shows the effect of adding core to the mantle, with the numbers giving the percentage of core in the mixture. The slope of the best-fit line through these data suggests that there has been less than 0.2% core addition to the mantle over the past 4 Ga. The dashed gray horizontal line shows the median Fe/Mn = 60.6 (n = 5,776). Data are from the EarthChem database (**http://www.earthchem.org/**).

et al. 1984). A carbonaceous chondrite late veneer, however, conflicts with the observation that carbonaceous chondrites have different Re/Os ratios (Walker & Morgan 1989) and Ru isotopic compositions (Fischer-Godde et al. 2013) from those of Earth's mantle. As Ru, Re, and Os in the mantle are all dominated by the late veneer, this observation appears to rule out carbonaceous chondrites as the main late-accreting material added to Earth after core formation.

4. HEALING AND TRANSITION TO A RECOGNIZABLE WORLD

Following the last giant impact into Earth, the planet had a core of similar size to the present core, but the chemical structure of the silicate portion of the planet is largely conjectural. By 4.36 Ga, surface conditions on Earth had reached the point where relatively low-temperature melting (Watson & Harrison 2005) of hydrous altered rocks (Mojzsis et al. 2001, Valley et al. 2002) was producing granitoid melts that crystallized the zircons now found as a small detrital component in quartzites in western Australia. The observational data thus suggest that Earth

somehow arrived at a structural, compositional, and dynamic state not dramatically different from the modern Earth within only a few hundred million years of Earth formation. How it made this transition is only now beginning to be revealed.

4.1. Erasing the Magma Ocean Signature from Earth's Mantle

Regardless of the details of magma ocean crystallization, only in the unlikely situation that there was no separation of crystals from liquid would the mantle be expected to be homogeneous. There are two timescales for characterizing the evolution of the mantle heterogeneity left from magma ocean crystallization that provide a guide for interpreting geochemical measurements and present seismological observations. First is the dispersion timescale t_d over which regions with distinct major or trace element compositions will be scattered throughout the mantle. The dispersion timescale is inversely proportional to the strain rate. Second is the mixing timescale over which these regions will be stretched and thinned within the convecting mantle. The reduction in length scale of heterogeneity is dominated by pure shear in chaotic flows, which leads to exponential stretching in time (Ottino 1990). For a mean mantle strain rate of 10^{-15} s^{-1}, heterogeneity with a dimension of 1,000 km will be reduced to 100 km after 72 Ma and a seismologically difficult-to-image 1 km after 220 Ma (Olson et al. 1984). The time to reduce length scales to the point that diffusion becomes important, the mixing time t_m, is proportional to $\dot{e}^{-1} \log(\dot{e} a_0^2 / D)$, where $\dot{e}$ is strain-rate, a_0 is the initial length scale, and D is diffusivity (Kellogg & Turcotte 1987). Thus, t_m is dominated by convection and is much less sensitive to diffusivity; 5–10 mantle overturns are sufficient for homogenization (Huber et al. 2009). For typical mantle strain rates and diffusivities, t_d is much shorter that t_m, implying that heterogeneity will be dispersed throughout the mantle before diffusion becomes important (Coltice & Schmalzl 2006).

For conditions representative of the early Earth, mixing times were probably <100 Ma (Coltice & Schmalzl 2006). Longer-term preservation of heterogeneity created during accretion and earliest differentiation thus requires that heterogeneity is not passively advected by flow in the mantle, but instead actively interacts with the flow. Heterogeneities that are mechanically strong, owing to differences in composition or grain size, could persist for billions of years if they are a couple of orders of magnitude more viscous than the surrounding mantle (Manga 1996). Density contrasts would also serve to isolate heterogeneity from the bulk of the convecting mantle, and there are plausible combinations of density and viscosity contrasts that could allow compositionally distinct layers to persist for the age of Earth (Le Bars & Davaille 2004).

Although convection homogenizes Earth's interior, it is also a source of heterogeneity: Upwelling mantle melts and hence extracts volatiles and other incompatible elements from the mantle. Convection also entrains material from the surface (and any other compositionally distinct region) into the mantle. At present, subduction is commonly assumed to be the dominant source of chemical heterogeneity in the mantle (Stixrude & Lithgow-Bertelloni 2012). As a result, there are a range of timescales for creating and erasing mantle heterogeneity, and each timescale, when constrained by observations, offers a window into early Earth processes. One example is the secular increase in platinum group element (PGE) concentrations in Archean komatiites between at least 3.6 and 2.9 Ga (Maier et al. 2009). The monotonic increase over this time period (much longer than the dispersion time) implies a source of PGEs that is added to the mantle from some reservoir; Maier et al. (2009) proposed mixing of late-accreted meteoritic material into the mantle, presumably by entrainment of early crust over a 0.7 Ga timescale. At any given time, however, the variability of PGE concentrations is small, consistent with much shorter (<100 Ma) mixing timescales within the early mantle.

A similar conclusion is suggested by the recent observation of tungsten (W) isotope variability in Archean rocks (Willbold et al. 2011, Touboul et al. 2012). The W isotope anomalies are created by the 9 Ma half-life radioactive decay of ^{182}Hf. Core formation will leave the mantle with a very high Hf/W ratio as a result of the extraction of the siderophile W into the core but retention of lithophile Hf in the mantle. The higher-than-chondritic ^{182}W/^{184}W ratio of Earth's modern mantle indicates that core formation on Earth started while ^{182}Hf was still extant (Kleine et al. 2009). The even higher ^{182}W/^{184}W ratio seen in some Archean rocks may sample a section of mantle that had been depleted in W by core formation, but that had not yet had chondritic W added back by late-accreting material. A similar diminution of early-formed mantle heterogeneity can be inferred from the observed variability of ^{142}Nd/^{144}Nd in mantle-derived rocks from 3.8 to 2.7 Ga (Bennett et al. 2007, Carlson & Boyet 2008, Debaille et al. 2013). As ^{142}Nd is produced by the decay of 68 Ma half-life ^{146}Sm, the variability in ^{142}Nd/^{144}Nd in some Archean rocks must reflect chemical differentiation events that occurred in their mantle source regions prior to ~4.4 Ga (Caro 2011, Rizo et al. 2011). Because mantle Nd abundances are similar to chondritic, unlike the HSEs and W, Nd in Earth's mantle is not sensitive to the late addition of extraterrestrial material. Thus, the diminution of ^{142}Nd variation throughout the Archean must reflect homogenization of either ancient crust or mantle heterogeneities created during early differentiation of the silicate Earth.

Another signature of early mantle chemical differentiation is seen in the isotopic composition of Xe in the mantle. ^{129}Xe is produced from the decay of ^{129}I (half-life of 15.7 Ma). The recent realization that the lower ^{129}Xe/^{130}Xe ratio in plumes compared with MORBs cannot be explained solely by mixing recycled atmospheric Xe with MORB-type Xe indicates that the different ^{129}Xe/^{130}Xe ratios in plumes and MORBs result from distinct mantle outgassing rates for their different mantle source reservoirs while ^{129}I was still alive; i.e., within the first 100 Ma of Solar System history (Mukhopadhyay 2012, Peto et al. 2013). Unlike W and Nd, the signature of the early differentiation is still preserved in the present-day Xe isotopic composition of the plume and MORB source reservoirs in the mantle. This is likely due to the low recycling efficiency into the mantle of the noble gases, which, once outgassed from the mantle, mostly reside in Earth's atmosphere. In contrast, the lithophile elements, like Nd, are concentrated in crustal rocks that can be returned to the mantle via plate subduction.

4.2. Earth's First Crust

The nature of Earth's first crust is unclear. Speculations range from a quasi-stable quench crust of peridotitic/komatiitic composition (Smith 1981) to a very evolved composition approaching tonalite (Harrison 2009). The oldest terrestrial materials, dated at 4.36 to 4.40 Ga, are detrital zircon grains in Archean quartzites from Western Australia (Froude et al. 1983, Mojzsis et al. 2001, Wilde et al. 2001, Holden et al. 2009). The mineral inclusion suite (Hopkins et al. 2008) and elevated δ^{18}O (Mojzsis et al. 2001, Valley et al. 2002) in a portion of the Hadean zircon suite are interpreted to indicate their derivation from broadly granitic rocks that were formed by relatively low pressure and temperature wet melting of a sedimentary or altered igneous precursor (Harrison 2009). The oldest rocks dated by using U-Pb isotopic measurements in the zircons they contain are just over 4.0 Ga, with one xenocrystic zircon core of 4.2 Ga (Iizuka et al. 2006); these are metatonalites and metagranodiorites from the Acasta terrane of central Canada (Bowring et al. 1990, Bowring & Williams 1999, Iizuka et al. 2007). As these types of silica-rich rocks cannot be derived directly by melting of mantle peridotite, but instead are produced from either extensive differentiation of basaltic magmas or remelting of hydrated basalt, neither the Hadean zircon source nor the Acasta gneisses are likely to represent Earth's first crust.

Many models for Archean continent formation produce the silica-rich tonalite-trondhjemite-granodiorite (TTG) suite by remelting thick, hydrothermally altered, basaltic crust, for example a basaltic plateau whose modern analog may be something like the Ontong Java Plateau (Kamber et al. 2005, Kemp et al. 2010). Two areas of ancient crust have compositional characteristics similar to those expected for such basaltic crust—the Isua supracrustal sequence of Greenland (Nutman et al. 1997b) and the Nuvvuagittuq supracrustal rocks of northern Quebec (O'Neil et al. 2007, O'Neil et al. 2011). The Isua rocks are dated at 3.7 to 3.8 Ga (Nutman et al. 1997a). Similarly, intrusive TTG rocks in the Nuvvuagittuq belt have zircon ages near 3.8 Ga (David et al. 2009, Cates & Mojzsis 2007), which sets a minimum age for the belt. The metavolcanic rocks in Nuvvuagittuq, however, provide ^{146}Sm-^{142}Nd whole-rock isochron ages of 4.3 to 4.4 Ga that reflect either the age of their formation (O'Neil et al. 2012) or mixing of 3.8 Ga igneous rocks with a ∼4.4 Ga material, perhaps preexisting crust (Roth et al. 2013). The Nuvvuagittuq metavolcanic rocks, now highly metamorphosed, suggest igneous protoliths similar to those seen in modern convergent margin volcanic arcs (O'Neil et al. 2011) where mantle melting is instigated by the transport of water into the mantle by the subducting crust. These most ancient examples of terrestrial crust thus appear to be related not to magma ocean processes but instead to shallow mantle melting similar to that occurring today. The composition of these ancient mafic rocks thus is in accord with the indications from the mineral inclusions in the Australian Hadean zircons (Hopkins et al. 2008) that the thermal gradient in at least the uppermost mantle at 4.36 to 3.8 Ga was not too dissimilar to the low gradient observed in modern convergent margins. The oxygen isotope variability in the Hadean zircons (Mojzsis et al. 2001, Valley et al. 2002), along with the presence of pillow basalts and chemical sediments in the oldest supracrustal belts (Appel et al. 1998, O'Neil et al. 2012), shows that Earth's surface had cooled to the point that liquid water was present, at least intermittently, by as early as 4.3 Ga.

5. FEATURES LEFT FROM THE EARLY EARTH

The most obvious remnant of early Earth differentiation that survives to the present is the core. Another is Xe in Earth's atmosphere and mantle, where radiogenic ^{129}Xe points to the separation of the atmosphere from the solid Earth by ∼4.45 Ga (Staudacher & Allegre 1982, Pepin & Porcelli 2006) accompanied by formation of distinct ocean island basalt and mid-ocean basalt mantle source reservoirs (Mukhopadhyay 2012).

Evidence for early mantle differentiation from elements other than the noble gases suggests an initially heterogeneous mantle, but a diminution of that heterogeneity from 3.8 to 2.7 Ga that may reflect convective mixing in the mantle. Whether or not mantle convection erased all initial lithophile element heterogeneity in the mantle is not yet clear. A difference in ^{142}Nd/^{144}Nd ratio between average ordinary and carbonaceous chondrites and all terrestrial rocks was suggested as evidence for an early Earth differentiation event and long-term isolation of an incompatible element–rich reservoir at the base of the mantle (Boyet & Carlson 2005). Others suggest that this difference reflects a nonchondritic composition for the bulk Earth (O'Neill & Palme 2008, Caro & Bourdon 2010). The interpretation is further complicated by the observation of nucleosynthetic anomalies in Nd (Carlson et al. 2007, Andreasen & Sharma 2007, Qin et al. 2011) that can cause variability of ^{142}Nd/^{144}Nd ratios independent of contributions from the radioactive decay of ^{146}Sm. The latter two explanations do not require an isolated incompatible element–enriched reservoir in the mantle.

The increasing resolution of seismic images of structures at the base of the mantle does suggest features that may be chemically distinct from the surrounding mantle. Whether these are remnants of early Earth differentiation or the graveyard of subducted oceanic plates, however,
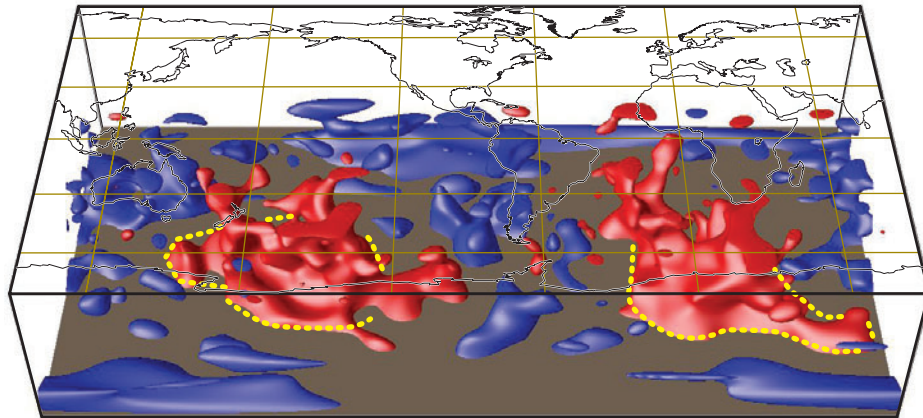
Figure 7

Seismic shear velocities in the lower mantle isocontoured at the +/−0.6% level for the model S20RTS
(Ritsema et al. 2004). Red and blue regions represent lower- and higher-than-average velocities, respectively.
Yellow dashed lines represent regions where body wave analyses demonstrate sharp transitions between the
large low shear velocity provinces and the surrounding mantle. After Garnero & McNamara (2008).

is not yet resolved. The latter possibility requires collecting subducted material in a way that
prevents its entrainment in viscous mantle flow. Seismic studies have long identified a spher-
ical harmonic degree-two pattern of seismic velocity variation in the lowermost lower mantle
(**Figure 7**) (Dziewonski et al. 1977, Dziewonski 1984). Seismically fast regions (i.e., the circum-
Pacific anomalies) correspond well with the extrapolation of surface subduction zones to the
core-mantle boundary, whereas the seismically slow anomalies [large low shear velocity provinces
(LLSVPs; Garnero & McNamara 2008)] seen in the central South Pacific and South Atlantic
under Africa are in the regions away from modern subduction and are instead below hot-spot
volcanism (Thorne & Garnero 2004). This is consistent with the notion in a whole-mantle con-
vection model that large-scale mantle structure is controlled by plate tectonic motions (Hager
& O'Connell 1981). As much as 90% of the long-wavelength geoid anomalies can be explained
by flow models in which the long-wavelength seismic structures in the lower mantle are treated
as density anomalies (Ricard et al. 1984, Hager & Richards 1989). Furthermore, these studies
showed that the long-wavelength geoid observations cannot be explained by mantle flow mod-
els with compositionally distinct upper and lower mantles, thus strongly favoring a whole-mantle
convection model with a uniform mantle composition. Ricard et al. (1993) and Lithgow-Bertelloni
& Richards (1998) showed that a model tracking the penetration of subducted slabs into the lower
mantle over the past 120 Ma well explained the long-wavelength fast seismic structures in the
lower mantle as well as the geoid, an explanation that was supported by regional and global geody-
namic modeling of mantle convection (Bunge et al. 1998, Bunge & Grand 2000). Small chemical
differences between the upper and lower mantle, however, cannot yet be ruled out, and whole-
mantle convection does not require simple undisturbed flow through the mantle. Seismic evidence
increasingly points to different fates of subducted oceanic plates as they travel into the transition
zone; some stagnate in the transition zone or in the uppermost lower mantle, whereas others flow
largely unhindered into the deep lower mantle (van der Hilst & Karason 1999, Fukao & Obayashi
2013). Hence, flow across the 660-km discontinuity is impeded, but not stopped (Dziewonski
et al. 2010). Such a phenomenon, coupled with the much higher viscosity of the lower mantle
compared with the upper mantle, may lead to faster processing and mixing of the upper mantle

(Gonnermann & Mukhopadhyay 2009), which could produce subtle differences in the chemical composition and particularly the size scale of chemical heterogeneity between the upper and lower mantle (van Keken et al. 2002).

Interpretation of the seismically slow structures in the lowermost mantle, however, is not as clear. The total volume of the two LLSVPs is of order ∼1–2% of the mantle depending on the precise boundaries and heights chosen for the LLSVPs (He & Wen 2012). One view is that these are slightly warmer mantle that has not been cooled by recent subducted slabs (Davies & Richards 1992, Davies et al. 2012), but this explanation may be inconsistent with the large variations in seismic wave speed and strong attenuation associated with these structures in the middle mantle (Ritsema et al. 1998, Romanowicz & Gung 2002). In addition, the shear wave and bulk sound speeds for the two LLSVPs are anticorrelated in places, suggesting that the LLSVPs may have a distinct composition from the surrounding mantle (Su & Dziewonski 1997, Masters et al. 2000). Thin (up to 40 km thick) patches of ULVZs are reported in multiple locations in the LLSVPs at the core-mantle boundary (Garnero & Helmberger 1996, Thorne & Garnero 2004), and their large reduction in seismic speeds suggests the existence of partial melt or/and compositional differences (Williams & Garnero 1996). Studies of seismic waveforms for waves grazing the boundaries of the LLSVPs show that the seismic speed variations across the boundaries are too rapid to be of a purely thermal origin, thus supporting the inference that the LLSVPs have a distinct composition (Wen et al. 2001, Ni et al. 2002, To et al. 2005, Wang & Wen 2007). The waveform modeling studies suggest that the side boundaries of LLSVPs are sharp, and in some places may be nearly vertical and rise up to hundreds of kilometers above the core-mantle boundary (Ni et al. 2002, Wang & Wen 2007).

If the LLSVPs are made of material separated from the rest of the mantle early in Earth history, to maintain their dynamic stability against mantle overturn, their compositional negative buoyancy must outweigh their thermal buoyancy (Davaille 1999, Kellogg et al. 1999). Treating the LLSVPs as compositionally distinct and negatively buoyant materials, thermochemical mantle convection models show that plate motion history may be responsible for generating the configurations of the African and Pacific LLSVPs (McNamara & Zhong 2005, Bull et al. 2009). These models demonstrate that cold mantle downwellings push away hot chemical piles at the core-mantle boundary (Jellinek & Manga 2002), thus controlling the configuration and structure of the LLSVPs.

If LLSVPs are the source of primitive noble gases seen in plume-derived ocean island basalts, then according to their Xe isotopic signature, the LLSVPs must have formed prior to 4.45 Ga (Mukhopadhyay 2012, Peto et al. 2013). If so, the LLSVPs also could represent the isolated incompatible element–rich reservoir that may explain the difference in modern accessible mantle $^{142}Nd/^{144}Nd$ ratio compared with that of most chondrites. In this case, however, the constancy of the $^{142}Nd/^{144}Nd$ ratio of mantle-derived rocks over the past 2.7 Ga requires that entrainment of LLSVP material into general mantle circulation must be less than 2% to 14% of their present mass (Jackson et al. 2010).

The degree-two structure dominates the large-scale structure and dynamics of the lowermost mantle at present. The extent to which this has always been the case is unclear. Two different proposals have emerged. On the basis of the spatial correlation of large igneous provinces, hot-spot volcanism, and kimberlite volcanism with the boundaries of the two LLSVPs (Burke & Torsvik 2004, Thorne et al. 2004), Burke et al. (2008) and Torsvik et al. (2010) suggested that the African and Pacific LLSVPs may have been stable spatially for at least 500 Ma. This is consistent with the observation that the equatorial degree-two position at the base of the mantle associated with the LLSVPs corresponds to a stable configuration from the point of view of Earth's moment of inertia (Dziewonski et al. 2010, Rouby et al. 2010). Indeed, true polar wander has been confined, for at least the past 200 Ma, to the meridional ring of fast velocities that separates the two LLSVPs,

suggesting an upside-down view of tectonics in which the LLSVPs, formed early in Earth history, might exert some stabilizing control on the location of subduction (Dziewonski et al. 2010). In contrast, on the basis of the dynamics of the supercontinent Pangea, Zhong et al. (2007) and Zhang et al. (2010) proposed that the African LLSVP may not have existed until significantly after 330 Ma, when Pangea formed. During much of the Paleozoic, deep mantle structure may have been predominantly degree-one with only one LLSVP (i.e., the Pacific one). Whether or not the LLSVPs are remnants of early Earth differentiation, resolving their true nature will help define their potential role in such critical Earth processes as the history of large-volume volcanic events (Burke et al. 2008), continental vertical motions (Zhang et al. 2010), and the geomagnetic field (Olson et al. 2013).

6. SUMMARY

The processes of planet formation are responsible for the first-order features of Earth: its bulk composition and separation into core, mantle, and atmosphere. The density and viscosity contrast of core and mantle appear to have been sufficient to keep material transport between core and mantle to a minimum over Earth history. For the other layers of Earth, however, post–core formation additions of material along with mass exchange between layers likely have dramatically modified their starting compositions. Evidence for global differentiation of the silicate Earth accompanying Earth's formation is remarkably muted compared to that for the Moon and Mars. Whether this reflects the many gaps in our understanding of how a thousand-kilometer or deeper magma ocean would evolve, or instead reflects the overprinting of 4.5 billion years of the stirring caused by mantle convection and plate tectonics, is not yet clear. Advances in our knowledge of material properties under the pressure and temperature conditions of the deep mantle and core will enable more stringent tests of thermal and compositional models against seismic observations and dynamic simulations. As geochronologic techniques increasingly see more clearly through later metamorphic effects to find Earth's oldest rocks, the results paint a picture of an early Earth remarkably similar to the current Earth in its surface and shallow interior thermal profile and the geologic processes that were operating to create continental crust and modify the composition of the mantle. Seeking evidence for early Earth differentiation requires looking back to the earliest part of Earth history, or to the deepest parts of the mantle. Resolution of the properties and origin of the seismically anomalous portions of the deep mantle may eventually provide key information on whether remnants of early Earth differentiation still survive in Earth's interior and how these might influence the geologic evolution of the surface of our home planet.

modeling results of Cuk & Stewart (2012). The CIDER Summer Program was supported by NSF-FESD-1135452.

LITERATURE CITED

Allegre CJ, Mahnes G, Gopel C. 2008. The major differentiation of the Earth at ~4.45 Ga. *Earth Planet. Sci. Lett.* 267:353–64

Amelin Y. 2008. U-Pb ages of angrites. *Geochim. Cosmochim. Acta* 72:221–32

Andrault D, Bolfan-Casanova N, Nigro GL, Bouhifd MA, Garbarino G, Mezouar M. 2011. Solidus and liquidus profiles of chondritic mantle: implication for melting of the Earth across its history. *Earth Planet. Sci. Lett.* 304:251–59

Andrault D, Petitgirard S, Nigro SL, Devidal J-L, Garbarino G, Mezouar M. 2012. Solid-liquid iron partitioning in Earth's deep mantle. *Nature* 487:354–57

Andreasen R, Sharma M. 2007. Mixing and homogenization in the early solar system: clues from Sr, Ba, Nd, and Sm isotopes in meteorites. *Astrophys. J.* 665:874–83

Appel PWU, Fedo CM, Moorbath S, Myers JS. 1998. Recognizable primary volcanic and sedimentary features in a low-strain domain of the highly deformed, oldest known (~3.7–3.8 Gyr) greenstone belt, Isua, West Greenland. *Terra Nova* 10:57–62

Asphaug E, Agnor CB, Williams Q. 2005. Hit-and-run planetary collisions. *Nature* 439:155–60

Bennett VC, Brandon AD, Nutman AP. 2007. Coupled [142]Nd-[143]Nd isotopic evidence for Hadean mantle dynamics. *Science* 318:1907–10

Benz W, Slattery WL, Cameron AGW. 1988. Collisional stripping of Mercury's mantle. *Icarus* 74:516–28

Borg LE, Connelly JN, Boyet M, Carlson RW. 2011. Chronological evidence that the Moon is either young or did not have a global magma ocean. *Nature* 477:70–73

Borg LE, Draper DS. 2003. A petrogenetic model for the origin and compositional variation of the Martian basaltic meteorites. *Meteorit. Planet. Sci.* 38:1713–31

Bouhifd MA, Jephcoat AP. 2011. Convergence of Ni and Co metal-silicate partition coefficients in the deep magma-ocean and coupled silicon-oxygen solubility in iron melts at high pressures. *Earth Planet. Sci. Lett.* 307:341–48

Bowring SA, Housh TB, Isachsen CE. 1990. The Acasta gneisses; remnant of Earth's early crust. In *The Origin of the Earth*, ed. HE Newsom, JH Jones, pp. 319–43. New York: Oxford Univ. Press

Bowring SA, Williams IS. 1999. Priscoan (4.00–4.03 Ga) orthogneisses from northwestern Canada. *Contrib. Mineral. Petrol.* 134:3–16

Boyet M, Blichert-Toft J, Rosing M, Storey M, Telouk P, Albarede F. 2003. [142]Nd evidence for early Earth differentiation. *Earth Planet. Sci. Lett.* 214:427–42

Boyet M, Carlson RW. 2005. [142]Nd evidence for early (>4.53 Ga) global differentiation of the silicate Earth. *Science* 309:576–81

Boyet M, Carlson RW. 2007. A highly depleted moon or a non-magma ocean origin for the lunar crust? *Earth Planet. Sci. Lett.* 262:505–16

Brandon AD, Lapen TJ, Debaille V, Beard BL, Rankenburg K, Neal C. 2009. Re-evaluating [142]Nd/[144]Nd in lunar mare basalts with implications for the early evolution and bulk Sm/Nd of the Moon. *Geochim. Cosmochim. Acta* 73:6421–45

Brandon AD, Walker RJ. 2005. The debate over core-mantle interaction. *Earth Planet. Sci. Lett.* 232:211–25

Brenan JM, McDonough WF. 2009. Core formation and metal-silicate fractionation of osmium and iridium from gold. *Nat. Geosci.* 2:798–801

Bull AL, McNamara AK, Ritsema J. 2009. Synthetic tomography of plume clusters and thermochemical piles. *Earth Planet. Sci. Lett.* 278:152–62

Bunge HP, Grand SP. 2000. Mesozoic plate-motion history below the northeast Pacific Ocean from seismic images of the subducted Farallon slab. *Nature* 405:337–40

Bunge HP, Richards MA, Lithogow-Bertelloni C, Baumgardner JR, Grand SP, Romanowicz BA. 1998. Time scales and heterogeneous structure in geodynamic Earth models. *Science* 280:91–95

Burke K, Steinberger B, Torsvik TH, Smethurst MA. 2008. Plume generation zones at the margins of large low shear velocity provinces on the core-mantle boundary. *Earth Planet. Sci. Lett.* 265:49–60

Burke K, Torsvik TH. 2004. Derivation of large igneous provinces of the past 200 million years from long-term heterogeneities in the deep mantle. *Earth Planet. Sci. Lett.* 227:531–38

Burkemper LK, Agee CB, Garcia KA. 2012. Constraints on core formation from molybdenum solubility in silicate melts at high pressure. *Earth Planet. Sci. Lett.* 335–36:95–104

Burkhardt C, Kleine T, Oberli F, Pack A, Bourdon B, Wieler R. 2011. Molybdenum isotope anomalies in meteorites: constraints on solar nebula evolution and origin of the Earth. *Earth Planet. Sci. Lett.* 312:390–400

Canup RM. 2004. Simulations of a late lunar-forming impact. *Icarus* 168:433–56

Canup RM. 2012. Forming a moon with an Earth-like composition via a giant impact. *Science* 338:1052–55

Carlson RW, Boyet M. 2008. Composition of Earth's interior: the importance of early events. *Philos. Trans. R. Soc. A* 366:4077–103

Carlson RW, Boyet M, Horan M. 2007. Chondrite barium, neodymium, and samarium isotopic heterogeneity and early Earth differentiation. *Science* 316:1175–78

Carlson RW, Lugmair GW. 1979. Sm-Nd constraints on early lunar differentiation and the evolution of KREEP. *Earth Planet. Sci. Lett.* 45:123–32

Caro G. 2011. Early silicate Earth differentiation. *Annu. Rev. Earth Planet. Sci.* 39:31–58

Caro G, Bourdon B. 2010. Non-chondritic Sm/Nd ratio in the terrestrial planets: consequences for the geochemical evolution of the mantle-crust system. *Geochim. Cosmochim. Acta* 74:3333–49

Caro G, Bourdon B, Birck JL, Moorbath S. 2006. High-precision $^{142}Nd/^{144}Nd$ measurements in terrestrial rocks: constraints on the early differentiation of the Earth's mantle. *Geochim. Cosmochim. Acta* 70:164–91

Caro G, Bourdon B, Wood BJ, Corgne A. 2005. Trace-element fractionation in Hadean mantle generated by melt segregation from a magma ocean. *Nature* 436:246–49

Catalli K, Shim SH, Prakapenka VB. 2009. Thickness and Clapeyron slope of the post-perovskite boundary. *Nature* 462:782–85

Cates NL, Mojzsis SJ. 2007. Pre-3750 Ma supracrustal rocks from the Nuvvuagittuq supracrustal belt, northern Québec. *Earth Planet. Sci. Lett.* 255:9–21

Chambers JE. 2004. Planetary accretion in the inner Solar System. *Earth Planet. Sci. Lett.* 223:241–52

Chou C-L, Shaw DM, Crocket JH. 1983. Siderophile trace elements in the Earth's oceanic crust and upper mantle. *J. Geophys. Res.* 88:A507–18

Clayton RN, Grossman L, Mayeda TK. 1973. A component of primitive nuclear composition in carbonaceous meteorites. *Science* 182:485–88

Coltice N, Moreira M, Hernlund J, Labrosse S. 2011. Crystallization of a basal magma ocean recorded by helium and neon. *Earth Planet. Sci. Lett.* 308:193–99

Coltice N, Schmalzl J. 2006. Mixing times in the mantle of the early Earth derived from 2-D and 3-D numerical simulations. *Geophys. Res. Lett.* 33:L23304

Corgne A, Liebske C, Wood BJ, Rubie DC, Frost DJ. 2005. Silicate perovskite-melt partitioning of trace elements and geochemical signature of a deep perovskitic reservoir. *Geochim. Cosmochim. Acta* 69:485–96

Cuk M, Stewart ST. 2012. Making the Moon from a fast-spinning Earth: a giant impact followed by resonant despinning. *Science* 338:1047–52

Dauphas N, Marty B, Reisberg L. 2002. Molybdenum evidence for inherited planetary scale isotope heterogeneity of the protosolar nebula. *Astrophys. J.* 565:640–44

Dauphas N, Pourmand A. 2011. Hf-W-Th evidence for rapid growth of Mars and its status as a planetary embryo. *Nature* 473:489–93

Davaille A. 1999. Simultaneous generation of hot spots and superswells by convection in a heterogeneous planetary mantle. *Nature* 402:756–60

David J, Godin L, Stevenson R, O'Neil J, Francis D. 2009. U-Pb ages (3.8–2.7 Ga) and Nd isotope data from the newly identified Eoarchean Nuvvuagittuq supracrustal belt, Superior Craton, Canada. *GSA Bull.* 121:150–63

Davies DR, Goes S, Davies JH, Schuberth BSA, Bunge H-P, Ritsema J. 2012. Reconciling dynamic and seismic models of Earth's lower mantle: the dominant role of thermal heterogeneity. *Earth Planet. Sci. Lett.* 353:253–69

Davies GF, Richards MA. 1992. Mantle convection. *J. Geol.* 100:151–206

de Koker N, Karki BB, Stixrude L. 2013. Thermodynamics of the MgO-SiO$_2$ system in Earth's lowermost mantle from first principles. *Earth Planet. Sci. Lett.* 361:58–63

Debaille V, O'Neill C, Brandon AD, Haenecour P, Yin Q-Z, et al. 2013. Stagnant-lid tectonics in early Earth revealed by ^{142}Nd variations in late Archean rocks. *Earth Planet. Sci. Lett.* 373:83–92

Dorfman SM, Meng Y, Prakapenka VB, Duffy TS. 2013. Effects of Fe-enrichment on the equation of state and stability of (Mg,Fe)SiO$_3$ perovskite. *Earth Planet. Sci. Lett.* 361:249–57

Dziewonski AM. 1984. Mapping the lower mantle: determination of lateral heterogeneity in *P* velocity up to degree and order 6. *J. Geophys. Res.* 89(B7):5929–52

Dziewonski AM, Anderson DL. 1981. Preliminary reference Earth model (PREM). *Phys. Earth Planet. Inter.* 25:297–356

Dziewonski AM, Hager BH, O'Connell RJ. 1977. Large-scale heterogeneities in the lower mantle. *J. Geophys. Res.* 82:239–55

Dziewonski AM, Lekic V, Romanowicz B. 2010. Mantle anchor structure: an argument for bottom-up tectonics. *Earth Planet. Sci. Lett.* 299:69–79

Elkins-Tanton LT. 2008. Linked magma ocean solidification and atmospheric growth for Earth and Mars. *Earth Planet. Sci. Lett.* 271:181–91

Elkins-Tanton LT. 2012. Magma oceans in the inner solar system. *Annu. Rev. Earth Planet. Sci.* 40:113–39

Fiquet G, Auzende AL, Siebert J, Corgne A, Bureau H, et al. 2010. Melting of peridotite to 140 Gigapascals. *Science* 329:1516–18

Fischer-Godde M, Burkhardt C, Kleine T. 2013. Origin of the late veneer inferred from Ru isotope systematics. *Lunar Planet. Sci. Conf. Abstr.* 44:2876

Froude DO, Ireland TR, Kinny PD, Williams IS, Compston W, et al. 1983. Ion microprobe identification of 4100–4200 Myr old terrestrial zircons. *Nature* 304:616–18

Fukao Y, Obayashi M. 2013. Subducted slabs above, penetrating through, and trapped below the 660 km discontinuity. *J. Geophys. Res. Solid Earth* 188:1–19

Funamori N, Sato T. 2010. Density contrast between silicate melts and crystals in the deep mantle: an integrated view based on static-compression data. *Earth Planet. Sci. Lett.* 295:435–40

Garnero EJ, Helmberger DV. 1996. Seismic detection of a thin laterally varying boundary layer at the base of the mantle beneath the central-Pacific. *Geophys. Res. Lett.* 23:977–80

Garnero EJ, McNamara AK. 2008. Structure and dynamics of Earth's lower mantle. *Science* 320:626–28

Gonnermann HM, Mukhopadhyay S. 2009. Preserving noble gases in a convecting mantle. *Nature* 459:560–64

Hager BH, O'Connell RJ. 1981. A simple global model of plate dynamics and mantle convection. *J. Geophys. Res.* 86(B6):4843–67

Hager BH, Richards MA. 1989. Long-wavelength variations in Earth's geoid: physical models and dynamical implications. *Philos. Trans. R. Soc. A* 328:209–327

Halliday AN, Kleine T. 2005. Meteorites and the timing, mechanisms, and conditions of terrestrial planet accretion and early differentiation. In *Meteorites and the Early Solar System II*, ed. DS Lauretta, HY McSween Jr, pp. 775–801. Tucson: Univ. Ariz. Press

Harper CL, Jacobsen SB. 1996. Noble gases and Earth's accretion. *Science* 273:1814–18

Harrison TM. 2009. The Hadean crust: evidence from >4 Ga zircons. *Annu. Rev. Earth Planet. Sci.* 37:479–505

He Y, Wen L. 2012. Geographic boundary of the "Pacific Anomaly" and its geometry and transitional structure in the north. *J. Geophys. Res.* 117:B09308

Herndon JM. 1979. The nickel silicide inner core of the Earth. *Proc. R. Soc. A* 368:495–500

Holden P, Lanc P, Ireland TR, Harrison TM, Foster JJ, Bruce Z. 2009. Mass-spectrometric mining of Hadean zircons by automated SHRIMP multi-collector and single-collector U/Pb zircon age dating: the first 100,000 grains. *Int. J. Mass Spectrom.* 286:53–63

Hopkins M, Harrison TM, Manning CE. 2008. Low heat flow inferred from >4 Gyr zircons suggests Hadean plate boundary interactions. *Nature* 456:493–96

Huber C, Bachmann O, Manga M. 2009. Homogenization processes in silicic magma chambers by stirring and mushification (latent heat buffering). *Earth Planet. Sci. Lett.* 283:38–47

Iizuka T, Horie K, Komiya T, Maruyama S, Hirata T, et al. 2006. 4.2 Ga zircon xenocryst in an Acasta gneiss from northwestern Canada: evidence for early continental crust. *Geology* 34:245–48

Iizuka T, Komiya T, Ueno Y, Katayama I, Uehara Y, et al. 2007. Geology and zircon geochronology of the Acasta Gneiss Complex, northwestern Canada: new constraints on its tectonothermal history. *Precambr. Res.* 153:179–208

Jackson MG, Carlson RW, Kurz MD, Kempton PD, Francis D, Blusztajn J. 2010. Evidence for the survival of the oldest terrestrial mantle reservoir. *Nature* 466:853–56

Javoy M. 1995. The integral enstatite chondrite model of the Earth. *Geophys. Res. Lett.* 22:2219–22

Javoy M, Kaminski E, Guyot F, Andrault D, Sanloup C, et al. 2010. The chemical composition of the Earth: enstatite chondrite models. *Earth Planet. Sci. Lett.* 293:259–68

Jellinek AM, Manga M. 2002. The influence of a chemical boundary layer on the fixity and lifetime of mantle plumes. *Nature* 418:760–63

Jochum KP, Hofmann AW, Seufert HM. 1993. Tin in mantle-derived rocks: constraints on Earth evolution. *Geochim. Cosmochim. Acta* 57:3585–95

Kamber BS, Whitehouse MJ, Bolhar R, Moorbath S. 2005. Volcanic resurfacing and the early terrestrial crust: zircon U-Pb and REE constraints from the Isua Greenstone Belt, southern West Greenland. *Earth Planet. Sci. Lett.* 240:276–90

Kellogg LH, Hager BH, van der Hilst RD. 1999. Compositional stratification in the deep mantle. *Science* 283:1881–84

Kellogg LH, Turcotte DL. 1987. Homogenization of the mantle by convective mixing and diffusion. *Earth Planet. Sci. Lett.* 81:371–78

Kemp AIS, Wilde SA, Hawkesworth CJ, Coath CD, Nemchin A, et al. 2010. Hadean crustal evolution revisited: new constraints from Pb-Hf isotope systematics of the Jack Hills zircons. *Earth Planet. Sci. Lett.* 296:45–56

Kleine T, Touboul M, Bourdon B, Nimmo F, Mezger K, et al. 2009. Hf-W chronology of the accretion and early evolution of asteroids and terrestrial planets. *Geochim. Cosmochim. Acta* 73:5150–88

Labrosse S, Herlund JW, Coltice NA. 2007. A crystallizing dense magma ocean at the base of the Earth's mantle. *Nature* 450:866–69

Lay T, Garnero EJ, Williams Q. 2004. Partial melting in a thermo-chemical boundary layer at the base of the mantle. *Phys. Earth Planet. Inter.* 146:441–67

Le Bars M, Davaille A. 2004. Whole layer convection in a heterogeneous planetary mantle. *J. Geophys. Res.* 109:B03403

Lee C-T, Luffi P, Hoink T, Li J, Dasgupta R, Hernlund J. 2010. Upside-down differentiation and generation of a "primordial" lower mantle. *Nature* 463:930–33

Liebske C, Corgne A, Frost DJ, Rubie DC, Wood BJ. 2005. Compositional effects on element partitioning between Mg-silicate perovskite and silicate melts. *Contrib. Mineral. Petrol.* 149:113–28

Liebske C, Frost DJ. 2012. Melting phase relations in the MgO-$MgSiO_3$ system between 16 and 26 GPa: implications for melting in Earth's deep interior. *Earth Planet. Sci. Lett.* 345–48:159–70

Lithgow-Bertelloni C, Richards MA. 1998. The dynamics of Cenozoic and Mesozoic plate motions. *Rev. Geophys.* 36:27–78

Lodders K. 2003. Solar system abundances and condensation temperatures of the elements. *Astrophys. J.* 591:1220–47

Lugmair GW, Shukolyukov A. 1998. Early solar system timescales according to ^{53}Mn-^{53}Cr systematics. *Geochim. Cosmochim. Acta* 62:2863–86

Lyubetskaya T, Korenaga J. 2007. Chemical composition of Earth's primitive mantle and its variance. 1. Methods and results. *J. Geophys. Res.* 112:B03211

Maier WD, Barnes SJ, Campbell IH, Fiorentini ML, Peltonen P, et al. 2009. Progressive mixing of meteoritic veneer into the early Earth's deep mantle. *Nature* 460:620–23

Manga M. 1996. Mixing of heterogeneities in the mantle: effect of viscosity differences. *Geophys. Res. Lett.* 23:403–6

Mann U, Frost DJ, Rubie DC, Becker H, Audetat A. 2012. Partitioning of Ru, Rh, Pd, Re, Ir and Pt between liquid metal and silicate at high pressures and high temperatures—implications for the origin of the highly siderophile element concentrations in Earth's mantle. *Geochim. Cosmochim. Acta* 84:593–613

Masters G, Laske G, Bolton H, Dziewonski A. 2000. The relative behavior of shear velocity, bulk sound speed, and compressional velocity in the mantle: implications for chemical and thermal structure. In *Earth's Deep Interior: Mineral Physics and Tomography from the Atomic to the Global Scale*, ed. SI Karato A Forte, R Liebermann, G Masters, L Stixrude, pp. 63–87. Washington, DC: AGU

McDonough WF. 2003. Compositional model for the Earth's core. In *Treatise on Geochemistry*, Vol. 2: *The Mantle and Core*, ed. RW Carlson, pp. 547–68. Amsterdam: Elsevier

McDonough WF, Sun S. 1995. The composition of the Earth. *Chem. Geol.* 120:223–53

McKeegan KD, Kallio APA, Heber VS, Jarzebinski G, Mao PH, et al. 2011. The oxygen isotopic composition of the Sun inferred from captured solar wind. *Science* 332:1528–32

McNamara AK, Garnero EJ, Rost S. 2010. Tracking deep mantle reservoirs with ultra-low velocity zones. *Earth Planet. Sci. Lett.* 299:1–9

McNamara AK, Zhong S. 2005. Thermochemical structures beneath Africa and the Pacific Ocean. *Nature* 437:1136–39

Mojzsis SJ, Harrison TM, Pidgeon RT. 2001. Oxygen-isotope evidence from ancient zircons for liquid water at Earth's surface 4,300 Myr ago. *Nature* 409:178–80

Morgan JW, Walker RJ, Brandon AD, Horan MF. 2001. Siderophile elements in Earth's upper mantle and lunar breccias: data synthesis suggests manifestations of the same late influx. *Meteoritics Planet. Sci.* 36:1257–75

Mosenfelder JL, Asimow PD, Frost DJ, Rubie DC, Ahrens TJ. 2009. The $MgSiO_3$ system at high pressure: thermodynamic properties of perovskite, postperovskite, and melt from global inversion of shock and static compression data. *J. Geophys. Res.* 114:B01203

Mukhopadhyay S. 2012. Early differentiation and volatile accretion in deep mantle neon and xenon. *Nature* 486:101–4

Nemchin AA, Pidgeon RT, Whitehouse MJ, Vaughan JP, Meyer C. 2008. SIMS U-Pb study of zircon from Apollo 14 and 17 breccias: implications for the evolution of lunar KREEP. *Geochim. Cosmochim. Acta* 72:668–89

Ni S, Tan E, Gurnis M, Helmberger DV. 2002. Sharp sides to the African superplume. *Science* 296:1850–52

Nomura R, Ozawa H, Tateno S, Hirose K, Hernlund J, et al. 2011. Spin crossover and iron-rich silicate melt in the Earth's deep mantle. *Nature* 473:199–202

Nutman AP, Bennett VC, Friend CRL, Rosing MT. 1997a. ~3710 and >3790 Ma volcanic sequences in the Isua (Greenland) supracrustal belt; structural and Nd isotope implications. *Chem. Geol.* 141:271–87

Nutman AP, McGregor VR, Friend CRL, Bennett VC, Kinny PD. 1997b. The Itsaq gneiss complex of southern West Greenland; the world's most extensive record of early crustal evolution (3900–3600 Ma). *Precambr. Res.* 78:1–39

Nyquist LE, Shih CY. 1992. The isotopic record of lunar volcanism. *Geochim. Cosmochim. Acta* 56:2213–34

Nyquist LE, Wiesmann H, Bansal B, Shih CY, Keith JE, Harper CL. 1995. ^{146}Sm-^{142}Nd formation interval for the lunar mantle. *Geochim. Cosmochim. Acta* 59:2817–37

O'Brien DP, Morbidelli A, Levinson HF. 2006. Terrestrial planet formation with strong dynamical friction. *Icarus* 184:39–58

Olson P, Deguen R, Hinnov LA, Zhong S. 2013. Controls on geomagnetic reversals and core evolution by mantle convection in the Phanerozoic. *Phys. Earth Planet. Inter.* 214:87–103

Olson P, Yuen DA, Balsinger D. 1984. Convective mixing and fine-structure of mantle heterogeneity. *Phys. Earth Planet. Inter.* 36:291–304

O'Neil J, Carlson RW, Paquette J-L, Francis D. 2012. Formation age and metamorphic history of the Nuvvuagittuq greenstone belt. *Precambr. Res.* 220–21:23–44

O'Neil J, Francis D, Carlson RW. 2011. Implications of the Nuvvuagittuq greenstone belt for the formation of Earth's early crust. *J. Petrol.* 52:985–1009

O'Neil J, Maurice C, Stevenson RK, Larocque J, Cloquet C, et al. 2007. The geology of the 3.8 Ga Nuvvuagittuq (Porpoise Cove) greenstone belt, northeastern Superior Province, Canada. In *Earth's Oldest Rocks*, ed. MJ van Kranekdonk, RH Smithies, VC Bennett, pp. 219–54. Amsterdam: Elsevier

O'Neill HSC, Palme H. 2008. Collisional erosion and the non-chondritic composition of the terrestrial planets. *Philos. Trans. R. Soc. A* 366:4205–38

Ottino JM. 1990. Mixing, chaotic advection, and turbulence. *Annu. Rev. Fluid Mech.* 22:207–53

Pahlevan K, Stevenson DJ. 2007. Equilibration in the aftermath of the lunar-forming giant impact. *Earth Planet. Sci. Lett.* 262:438–49

Palme H, O'Neill HSC. 2003. Cosmochemical estimates of mantle composition. In *Treatise on Geochemistry*, Vol. 2: *The Mantle and Core*, ed. RW Carlson, HD Holland, KK Turekian, pp. 1–38. Amsterdam: Elsevier

Pepin RO. 1991. On the origin and early evolution of terrestrial planet atmospheres and meteoritic volatiles. *Icarus* 92:2–79

Pepin RO, Porcelli D. 2002. Origin of noble gases in the terrestrial planets. *Rev. Mineral. Geochem.* 47:191–246

Pepin RO, Porcelli D. 2006. Xenon isotope systematics, giant impacts, and mantle degassing on the early Earth. *Earth Planet. Sci. Lett.* 250:470–85

Peto M, Mukhopadhyay S, Kelley KA. 2013. Heterogeneities from the first 100 million years recorded in deep mantle noble gases from the Northern Lau back-arc basin. *Earth Planet. Sci. Lett.* 369–70:13–23

Qin L, Alexander CMOD, Carlson RW, Horan MF, Yokoyama T. 2010. Contributors to chromium isotope variation in meteorites. *Geochim. Cosmochim. Acta* 74:1122–45

Qin L, Carlson RW, Alexander CMOD. 2011. Correlated nucleosynthetic isotopic variability in Cr, Sr, Ba, Sm, Nd and Hf in Murchison and QUE 97008. *Geochim. Cosmochim. Acta* 75:7806–28

Regelous M, Elliott T, Coath CD. 2008. Nickel isotope heterogeneity in the early Solar System. *Earth Planet. Sci. Lett.* 272:330–38

Ricard Y, Fleitout L, Froidevaux C. 1984. Geoid heights and lithospheric stresses for a dynamic Earth. *Ann. Geophys.* 2:267–86

Ricard Y, Richards M, Lithogow-Bertelloni C, Stunff YL. 1993. A geodynamic model of mantle density heterogeneity. *J. Geophys. Res.* 98(B12):21895–909

Righter K. 2011. Prediction of metal-silicate partition coefficients for siderophile elements: an update and assessment of PT conditions for metal-silicate equilibrium during accretion of the Earth. *Earth Planet. Sci. Lett.* 304:158–67

Ritsema J, Ni S, Helmberger DV, Crotwell HP. 1998. Evidence for strong shear velocity reductions and velocity gradients in the lower mantle beneath Africa. *Geophys. Res. Lett.* 25:4245–48

Ritsema J, van Heijst HJ, Woodhouse JH. 2004. Global transition zone tomography. *J. Geophys. Res.* 109:B02302

Rizo H, Boyet M, Blichert-Toft J, Rosing M. 2011. Combined Nd and Hf isotope evidence for deep-seated source of Isua lavas. *Earth Planet. Sci. Lett.* 312:267–79

Romanowicz BA, Gung YC. 2002. Superplumes from the core-mantle boundary to the lithosphere: implications for heat-flux. *Science* 296:513–16

Rost S, Garnero EJ, Williams Q, Manga M. 2005. Seismological constraints on a possible plume root at the core-mantle boundary. *Nature* 435:666–69

Roth ASG, Bourdon B, Mojzsis SJ, Touboul M, Sprung P, et al. 2013. Inherited ^{142}Nd anomalies in Eoarchean protoliths. *Earth Planet. Sci. Lett.* 361:50–57

Rouby H, Greff-Lefftz M, Besse J. 2010. Mantle dynamics, geoid, inertia and TPW since 120 Myr. *Earth Planet. Sci. Lett.* 292:301–11

Rubie DC, Frost DJ, Mann U, Asahara Y, Nimmo F, et al. 2011. Heterogeneous accretion, composition and core-mantle differentiation of the Earth. *Earth Planet. Sci. Lett.* 301:31–42

Rubie DC, Melosh HJ, Reid JE, Liebske C, Righter K. 2003. Mechanisms of metal-silicate equilibration in the terrestrial magma ocean. *Earth Planet. Sci. Lett.* 205:239–55

Salters VJM, Stracke A. 2004. Composition of the depleted mantle. *Geochem. Geophys. Geosyst.* 5:Q05B07

Schonbachler M, Carlson RW, Horan MF, Mock TD, Hauri EH. 2010. Heterogeneous accretion and the moderately volatile element budget of Earth. *Science* 328:884–87

Seibert J, Badro J, Antonangeli D, Ryerson FJ. 2013. Terrestrial accretion under oxidizing conditions. *Science* 339:1194–97

Smith JV. 1981. The first 800 million years of Earth's history. *Philos. Trans. R. Soc. A* 301:401–22

Solomatov VS. 2000. Fluid dynamics of a terrestrial magma ocean. In *Origin of the Earth and Moon*, ed. RM Canup, K Righter, pp. 323–38. Tucson: Univ. Ariz. Press

Solomatov VS. 2007. Magma oceans and primordial mantle differentiation. In *Treatise on Geophysics*, Vol. 9: *Evolution of the Earth*, ed. DJ Stevenson, pp. 91–119. Amsterdam: Elsevier

Sramek O, McDonough WF, Kite ES, Lekic V, Dye ST, Zhong S. 2013. Geophysical and geochemical constraints on geoneutrino fluxes from Earth's mantle. *Earth Planet. Sci. Lett.* 361:356–66

Staudacher T, Allegre CJ. 1982. Terrestrial xenology. *Earth Planet. Sci. Lett.* 60:389–406

Stevenson DJ. 1987. Origin of the Moon—the collision hypothesis. *Annu. Rev. Earth Planet. Sci.* 15:271–315

Stevenson DJ. 1990. Fluid dynamics of core formation. In *Origin of the Earth*, ed. HE Newsom, JH Jones, pp. 231–49. New York: Oxford Univ. Press

Stixrude L, de Koker N, Sun N, Mookherjee M, Karki BB. 2009. Thermodynamics of silicate liquids in the deep Earth. *Earth Planet. Sci. Lett.* 278:226–32

Stixrude L, Lithgow-Bertelloni C. 2012. Geophysics of chemical heterogeneity in the mantle. *Annu. Rev. Earth Planet. Sci.* 40:569–95

Su W, Dziewonski AM. 1997. Simultaneous inversion for 3D variations in shear and bulk sound velocity in the mantle. *Phys. Earth Planet. Inter.* 100:135–56

Taylor DJ, McKeegan KD, Harrison TM. 2009. Lu-Hf zircon evidence for rapid lunar differentiation. *Earth Planet. Sci. Lett.* 279:157–64

Taylor SR, Jakes P. 1974. The geochemical evolution of the Moon. *Proc. Lunar Sci. Conf.* 5:1287–1305

Tera F, Wasserburg GJ. 1974. U-Th-Pb systematics on lunar rocks and inferences about lunar evolution and the age of the moon. *Proc. Lunar Sci. Conf.* 5:1571–99

Thomas CW, Liu Q, Agee CB, Asimow PD, Lange RA. 2012. Multi-technique equation of state for Fe_2SiO_4 melt and the density of Fe-bearing silicate melts from 0 to 161 GPa. *J. Geophys. Res.* 117:B10206

Thommes EW, Duncan MJ, Levinson HF. 2003. Oligarchic growth of giant planets. *Icarus* 161:431–55

Thorne MS, Garnero EJ. 2004. Inferences on ultralow-velocity zone structure from a global analysis of SPdKS waves. *J. Geophys. Res.* 109:B08301

Thorne MS, Garnero EJ, Grand S. 2004. Geographic correlation between hot spots and deep mantle lateral shear-wave velocity gradients. *Phys. Earth Planet. Inter.* 146:47–63

To A, Romanowicz B, Capdeville Y, Takeuchi N. 2005. 3D effects of sharp boundaries at the borders of the African and Pacific superplumes: observations and modeling. *Earth Planet. Sci. Lett.* 233:137–53

Tonks WB, Melosh HJ. 1993. Magma ocean formation due to giant impacts. *J. Geophys. Res.* 98(E3):5319–33

Torsvik TH, Burke K, Steinberger B, Webb SJ, Ashwal LD. 2010. Diamonds sampled by plumes from the core-mantle boundary. *Nature* 466:352–55

Touboul M, Kleine T, Bourdon B, Palme H, Wieler R. 2007. Late formation and prolonged differentiation of the Moon inferred from W isotopes in lunar metals. *Nature* 450:1206–9

Touboul M, Puchtel IS, Walker RJ. 2012. [182]W evidence for long-term preservation of early mantle differentiation products. *Science* 335:1065–69

Trinquier A, Birck J-L, Allegre CJ. 2007. Widespread [54]Cr heterogeneity in the inner solar system. *Astrophys. J.* 655:1179–85

Trinquier A, Birck J-L, Allegre CJ, Gopel C, Ulfbeck D. 2008. [53]Mn-[53]Cr systematics of the early Solar System revisited. *Geochim. Cosmochim. Acta* 72:5146–63

Trinquier A, Elliott T, Ulfbeck D, Coath C, Krot AN, Bizzarro M. 2009. Origin of nucleosynthetic isotope heterogeneity in the solar protoplanetary disk. *Science* 324:374–76

Tucker JM, Mukhopadhyay S, Schilling J-G. 2012. The heavy noble gas composition of the depleted MORB mantle (DMM) and its implications for the preservation of heterogeneities in the mantle. *Earth Planet. Sci. Lett.* 355–56:244–54

Valley JW, Peck WH, King EM, Wilde SA. 2002. A cool early Earth. *Geology* 30:351–54

van der Hilst RD, Karason H. 1999. Compositional heterogeneity in the bottom 1000 km of Earth's mantle: towards a hybrid convection model. *Science* 283:1885–88

van Keken PE, Hauri EH, Ballentine CJ. 2002. Mantle mixing: the generation, preservation, and destruction of chemical heterogeneity. *Annu. Rev. Earth Planet. Sci.* 30:493–525

Vervoort JD, Blichert-Toft J. 1999. Evolution of the depleted mantle: Hf isotope evidence from juvenile rocks through time. *Geochim. Cosmochim. Acta* 63:533–56

Wade J, Wood BJ. 2005. Core formation and the oxidation state of the Earth. *Earth Planet. Sci. Lett.* 236:78–95

Walker RJ. 2009. Highly siderophile elements in the Earth, Moon and Mars: update and implications for planetary accretion and differentiation. *Chem. Erde* 69:101–25

Walker RJ, Morgan JW. 1989. Rhenium-osmium systematics of carbonaceous chondrites. *Science* 243:519–22

Walsh KJ, Morbidelli A, Raymond SN, O'Brien DP, Mandell AM. 2011. A low mass for Mars from Jupiter's early gas-driven migration. *Nature* 475:206–9

Wang Y, Wen L. 2007. Geometry and P and S velocity structure of the "African Anomaly." *J. Geophys. Res.* 112:B05313

Wanke H, Baddenhausen H, Dreibus G, Jagoutz E, Kruse H, et al. 1973. Multielement analyses of Apollo 15, 16, and 17 samples and the bulk composition of the moon. *Proc. Lunar Sci. Conf.* 4:1461–81

Wanke H, Driebus G, Jagoutz E. 1984. Mantle chemistry and accretion history of the Earth. In *Archaean Geochemistry*, ed. A Kroner, GN Hanson, AM Goodwin, pp. 1–24. Berlin: Springer-Verlag

Warren PH. 2011. Stable-isotope anomalies and the accretionary assemblage of the Earth and Mars: a subordinate role for carbonaceous chondrites. *Earth Planet. Sci. Lett.* 311:93–100

Wasson JT, Kallemeyn GW. 1988. Composition of chondrites. *Philos. Trans. R. Soc. A* 325:535–44

Watson EB, Harrison TM. 2005. Zircon thermometer reveals minimum melting conditions on earliest Earth. *Science* 308:841–44

Wen L, Silver P, James D, Kuehnel R. 2001. Seismic evidence for a thermo-chemical boundary layer at the base of Earth's mantle. *Earth Planet. Sci. Lett.* 189:141–53

Wiechert U, Halliday AN, Lee D-C, Snyder GA, Taylor LA, Rumble DA. 2001. Oxygen isotopes and the Moon-forming giant impact. *Science* 294:345–48

Wilde SA, Valley JW, Peck WH, Graham CM. 2001. Evidence from detrital zircons for the existence of continental crust and oceans on Earth 4.4 Gyr ago. *Nature* 409:175–78

Willbold M, Elliott T, Moorbath S. 2011. The tungsten isotopic composition of the Earth's mantle before the terminal bombardment. *Nature* 477:195–98

Williams Q, Garnero EJ. 1996. Seismic evidence for partial melt at the base of Earth's mantle. *Science* 273:1528–30

Wood JA, Dickey JS Jr, Marvin UB, Powell BN. 1970. Lunar anorthosites and a geophysical model of the Moon. *Proc. Apollo 11 Lunar Sci. Conf.*, ed. AA Levinson, pp. 965–88. New York: Pergamon

Yokochi R, Marty B. 2004. A determination of the neon isotopic composition of the deep mantle. *Earth Planet. Sci. Lett.* 225:77–88

Zhang J, Dauphas N, Davis AM, Leya I, Fedkin A. 2012. The proto-Earth as a significant source of lunar material. *Nat. Geosci.* 5:251–55

Zhang N, Zhong SJ, Leng W, Li ZX. 2010. A model for the evolution of the Earth's mantle structure since the Early Paleozoic. *J. Geophys. Res.* 115:B06401

Zhong SJ, Zhang N, Li ZX, Roberts JH. 2007. Supercontinent cycles, true polar wander, and very long-wavelength mantle convection. *Earth Planet. Sci. Lett.* 261:443–55